

# Exploring the relationships between post-fire vegetation regeneration dynamics, topography and burn severity: A case study from the Montane Cordillera Ecozones of Western Canada

Gareth Ireland<sup>1</sup>, George P. Petropoulos\*

*Department of Geography and Earth Sciences, University of Aberystwyth, Old College, King Street, Llandinam Building, Room H4, Aberystwyth, Ceredigion, SY23 3DB, Wales, United Kingdom*

## ARTICLE INFO

### Article history:

Available online 26 December 2014

### Keywords:

Post-fire vegetation regeneration  
Topography  
Burn severity  
Landsat  
Remote sensing  
Canada

## ABSTRACT

In this study the relationships between vegetation regeneration dynamics to topography and burn severity for a Canadian landscape were investigated using freely available Earth Observation (EO) imagery from Landsat TM sensor. The Okanagan Mountain Park, located in the Montane Cordillera Ecozones of Western Canada at which a fire occurred in 2003, was used as a case study. First, vegetation regeneration dynamics were quantified for a period of 8 years following the fire event based on a chronosequence analysis of the Normalized Difference Vegetation Index (NDVI) and the Regeneration Index (RI). The spatio-temporal patterns of post-fire NDVI from each image date were statistically compared to the pre-fire pattern to determine the extent to which the pre-fire spatial pattern was re-established and also the rate of recovery. Subsequently, the relationships of vegetation regrowth to both topography and burn severity was quantified using a series of additional statistical metrics. Burn severity was derived from the differenced Normalized Burn Ratio (dNBR) index computed from the Landsat TM images. Information on topography properties of the region was obtained from the ASTER global operational product.

NDVI and RI analysis indicated a moderate vegetation recovery to pre-fire patterns, with regeneration to over 60% of the pre-fire levels 8-years after the fire. Regression analysis of pre- and post-fire mean NDVI exhibited significant re-growth in the first 3 years after the fire with a more gradual return in later years (an increase of 0.400 in  $R^2$  by 2006 compared to only an increase of 0.129 for the subsequent 5 years). Re-growth rates appeared to be somewhat higher in north-facing slopes in comparison to south facing ones. As expected, NDVI decline due to fire was positively correlated with burn severity class, whereas negative correlation was found between damage and regeneration ability (recovery after 3 years = low severity 64%/high severity 58%, recovery after 8 years = low severity 72%/high severity 70%). To our knowledge, this study is one of the few attempting to explore the interrelationships of post-fire vegetation regrowth, topography and burn severity, especially in the case of a single large fire. RI based on control plots provides a valuable tool to quantify fire impact and subsequent vegetation regrowth. Furthermore, indication of burn severity is useful for strategically rehabilitating areas of slow or unsuitable post-fire vegetation recovery. This study corroborates the significance of EO technology as a successful and cost-effective solution in providing information related to economic and environmental post-fire regeneration assessment.

© 2014 Elsevier Ltd. All rights reserved.

## Introduction

Fire is an integral part of many terrestrial ecosystems and is considered a natural phenomenon that has a fundamental role in their distribution, organisation and evolution (Arianoutsou,

Gimeno, Kazanis, Pausas, & Vallejo, 2007; Bowman et al., 2009; Koutsias et al., 2012). Fires can also be a major factor of disturbance which affects below ground physical, chemical and microbial processes, potentially altering successional rates, vegetation species composition, mineralisation rates and above ground biomass (Marozas, Racinskas, & Bartkevicius, 2007; Pausas, Lloret, Rodrigo, & Vallejo, 2008). These changes can dramatically affect land cover dynamics at a variety of spatial and temporal scales and can also have a potential impact on degradation processes, such as soil

\* Corresponding author. Tel.: +44 0 1970 621861.

E-mail addresses: [gai2@aber.ac.uk](mailto:gai2@aber.ac.uk) (G. Ireland), [gep9@aber.ac.uk](mailto:gep9@aber.ac.uk) (G.P. Petropoulos).

<sup>1</sup> Tel.: +44 0 1970 621861.

erosion, evapotranspiration and water runoff (Cawson, Sheridan, Smith, & Lane, 2013; Fox, Maselli, & Carrega, 2008). Many climate models have projected significant climate change by the end of this century due to the greenhouse effect (IPCC, 2007). This is expected to increase ecosystems susceptibility to wildfires, as well as increase the frequency, intensity, duration and timing of these disturbances. Increased fuel loads, longer fire seasons and the occurrence of more extreme weather conditions are all expected to contribute to increased wildfire activity (Mortsch, 2006).

Until very recently, post-fire recovery of burned landscapes occurred with little or no human intervention. However, in the past two decades, increased resource management and continued community development into fire-prone wildland areas has resulted in an increasing amount of research, management, and funding of post-fire stabilisation and rehabilitation to protect safety and other values at-risk (Robichaud, Lewis, Brown, & Ashmun, 2009). In this context, a number of post-fire rehabilitation programmes have been proposed. Those have predominantly aimed to determine the need for, and to prescribe and implement emergency treatments to minimise threats to life or property, or to stabilise and prevent further unacceptable degradation to natural and cultural resources resulting from the effects of a fire (NPS, Rehabilitation and Recovery, 2014). Such programmes are becoming more important as the ecological resources of wild land areas are recognised and valued, and the longer term consequences of post-fire treatments on the environment and ecological recovery are becoming more important in the post-fire treatment decision-making process (Robichaud et al., 2009). A number of post-fire techniques are used to decrease the potential hazard related to wildfires and also to promote the successful rehabilitation of the natural landscape. Prescribed burning or the thinning of trees are used to reduce fuels around facilities and towns, where types of vegetation, past fire behaviour, and terrain are all evaluated beforehand in order to ensure that the prescribed burning is safe, and meets ecological goals. Steep areas may need to be mulched for erosion control, whereas the monitoring and removal of exotic species, and selective planting could be necessary to encourage the return of native species. Archaeological sites and features may require mapping, stabilisation, or additional preservation work (NPS, Burned Area Restoration, 2014).

Given the high cost of many of these post-fire stabilisation and rehabilitation programmes and the time-frames associated with post-fire vegetation and soil recovery, which may take decades, it is not only important to monitor the effectiveness of their initial installation, but also to monitor their long term effectiveness. In this context, knowledge of the spatio-temporal distribution of post-fire vegetation recovery dynamics is of key importance to numerous aspects of policy and decision-making (Gouveia, DaCamara, & Trigo, 2010; Petropoulos, Griffiths, & Kalivas, 2014). Notably, two or three years after a fire, land management goals generally shift from stabilisation of burned areas to long-term productivity and ecological restoration (Robichaud et al., 2009). This is often more focused on the biotic components of the ecosystem, such as recovery of native communities and habitat, maintenance of biodiversity, re-establishment of timber or grazing species, and control of invasive weeds (Beschta et al., 2004; Casady, Leeuwen, & Marsh, 2009; Grissino-Mayer and Swetnam, 2000). Examining longer term post-fire vegetation regeneration dynamics thus allows for an understanding of the way different vegetation species respond naturally to fire, or if re-habilitated ecosystems developed through post-fire management programmes are functioning as desired (Naveh, 1991). Accurate information on post-fire vegetation recovery dynamics can also assist in identifying areas needing intensive or special restoration programs aiming to reduce soil erosion and runoff, thus mitigating long-term site degradation (Gouveia et al.,

2010; Malak and Pausas, 2006). Thus, it is understandable that the rate and spatial extent of vegetation recovery after fire can control the extent of various environmental, social, economic and political impacts (Minchella, Del Frate, Capogna, Anselmi, & Manes, 2009). If available in a consistent, repetitive and cost-effective manner, knowledge of post-fire vegetation dynamics is thus a crucial element of successful landscape management (Wittenberg, Malkinson, Beeri, Halutzy, & Tesler, 2007). Yet, both the spatial and temporal dynamics of post-fire recovery can vary significantly and are contingent upon a number of factors. This is because of the complexity of landscape structures and the responses of such systems to the diverse types of fire regimes (Pausas, Ribeiro, & Vallejo, 2004; Petropoulos et al., 2014).

Traditional methods to assess post-fire impact on vegetation are generally costly and labour intensive, and are frequently constrained by the broad spatial expanse and limited accessibility of areas affected by fire. The ensemble of Earth Observation (EO) and Geographic Information Systems (GIS) has shown to be a key framework in the extraction and analysis of spatial, spectral and temporal information related to vegetation regeneration dynamics monitoring (Chen, Chen, Liu, Li, & Tan, 2005; Kalivas, Petropoulos, Athanasiou, & Kollias, 2013). As a result, during the last two decades a considerable number of post-fire vegetation re-growth studies exploiting different types of EO data have been conducted at diverse ecosystems worldwide (Karaman, Özkelan, & Örmeci, 2011; Lunetta, Knight, Edirizwickrema, Lyon, & Worthy, 2006). However, the use of such systems to monitor long-term vegetation dynamics in the framework of post-fire rehabilitation and recovery programmes is limited.

Several image processing techniques have been explored in characterising post-fire vegetation recovery from optical EO data in particular. Some of the most widely used techniques include image classification (Karaman et al., 2011; Viedma, Meliá, Segarra, & García-Haro, 1997) and Spectral Mixture Analysis (Solans Vila and Barbosa, 2010; Veraverbeke et al., 2012). However, the use of spectral vegetation indices (VI) has evidently been the most extensively examined (Franks, Masek, & Turner, 2013; Hope, Albers, & Bart, 2012). Their use has largely been based on the hypothesis that the ratio of red (R) to near infrared (NIR) reflectance for green vegetation changes when the foliage containing chlorophyll is destroyed by the fire. Subsequently, the use of a spectral index that is sensitive to the R and NIR regions of the electromagnetic radiation spectrum can be used to identify and potentially quantify vegetation change.

The Normalised Difference Vegetation Index (NDVI, Rouse, Haas, Schell, & Deering, 1973) has perhaps been the most widely used index in vegetation regrowth studies. A significant number of studies have utilised this index to monitor post-fire vegetation dynamics in different ecosystems (Hope et al., 2012; Roder, Hill, Duguy, Alloza, & Vallejo, 2008). However, a much less utilised index used in this context is the so-called Regeneration Index (RI; Riaño, Chuvieco, Ustin, et al., 2002). For its computation, NDVI values between burned plots are compared to those unburned control plots within the same image that contained spectral and environmental characteristics similar to the state of the pre-fire burn scar area (Díaz-Delgado, Salvador, & Pons, 1998; Lhermitte, Verbesselt, Verstraeten & Coppin, 2007). As analysis of NDVI rates independently can cause the development of false trends in the data due to a wide range of noise factors that reduce the detection of regeneration patterns, this index essentially standardises multi-temporal measures of NDVI between the different EO images used based on these control plots. Thus, the control plots provide an analysis independent of possible radiometric calibration uncertainty, minor error in the atmospheric correction, topographic distortions, and phaeological differences in vegetation due to interannual or seasonal

differences (Riaño, Chuvieco, Salas, Palacios-Orueta, & Bastarrica, 2002; Riaño, Chuvieco, Ustin, et al., 2002). Although NDVI, and to a lesser extent RI (e.g. Lhermitte, Verbesselt, Verstraeten, & Coppin, 2010; Lhermitte, Verbesselt, Verstraeten, Veraverbeke, & Coppin, 2011; Riaño, Chuvieco, Ustin, et al., 2002), have been used to map vegetation regrowth, only a very limited number of studies have analysed the agreement between results of NDVI and RI for monitoring post-fire vegetation dynamics after the same fire event. In the absence of field data, the regeneration index based on control plots provides a valuable tool to quantify fire impact and subsequent vegetation regrowth, and is necessary to reduce image noise related to the use of NDVI alone. Noise reduction and correcting for phenological and seasonal changes are primary challenges associated with quantifying post-fire vegetation regeneration from multi-temporal imagery (Lhermitte et al., 2010; Song, Woodcock, & Li, 2002; Song, & Woodcock, 2003).

Several studies have expanded the use of VI's to study the effects of burn severity and fire intensity on ecosystems. A relatively new index is the Normalised Burn Ratio (NBR; Riaño, Chuvieco, Salas, et al. 2002). This is a ratio utilising the differing responses of vegetation to the NIR and shortwave infrared (SWIR) parts of electromagnetic radiation which are sensitive to changes in soil and vegetation moisture. Often, the NBR is calculated for both the pre-fire and post-fire satellite scenes, and then the two pre-/post-fire ratios are differenced (dNBR) to generate a scaled index, the application of which has shown to be an effective method to map burn severity for different land cover types (Norton, 2006; Pinno, Errington, & Thompson, 2013). Although dNBR is widely used in burn severity mapping studies, there is limited research into the use of this index to evaluate the relationship between burn severity and vegetation regrowth. This is important as dNBR can be a key factor to quantify fire impacts on vegetation and soil (De Santis and Chuvieco 2007; Van Wagendonk, Root, & Key, 2004; White, Ryan, Key, & Running, 1996) and to provide baseline information for monitoring restoration and recovery (Brewer et al., 2005). Indicators of burn severity, and thus potential ecosystem recovery, could prove useful to post-fire planners tasked with strategically rehabilitating areas likely to recover slowly or in undesirable ways (Lentile et al., 2007).

Topography also plays an important role in post-fire vegetation regeneration dynamics, where it is an important physiographic factor which affects vegetation recovery, as well as the fire proneness of an area. Aspect, is a key control on an area's microclimate, localised hydrological variability, and soil hydrophobicity, affecting vegetative growing conditions and also an area's susceptibility to fire (Karaman et al., 2011; Wimberly & Reilly, 2007). Unfortunately, interactions between topography and vegetation regeneration, as well as burn severity are poorly known, especially at the scale of a whole, large fire.

Very little work has been conducted examining and monitoring long-term post-fire vegetation recovery dynamics, particularly so in continental, hemi-boreal and montane ecosystems that are common in Western Canada (Schroeder et al., 2002; Ustin & Xiao, 2001). Moreover, research into the inter-relationship between vegetation recovery, topography and burn severity is severely limited. Yet, wildfires are a significant agent of land use/cover change in Canadian ecosystems (The Atlas of Canada, 2009). The amount of burn area across Canada has increased in the last few decades and is projected to be substantially higher by the end of the 21st century. This is attributed largely to factors related to climate change leading to a shifting of natural disturbance regimes, i.e. frequency and severity of natural disturbances and extreme weather events (IPCC, 2011; Rogers, Randerson, & Bonan, 2013).

In this context, we use the Okanagan Mountain Park Fire as a case study to quantify the dynamics of the regeneration process,

and quantitatively investigate the relationships between post-fire recovery and burn severity as well as topography, utilising multi-temporal analysis of Landsat TM imagery. Here it is examined if information provided by remote sensing on the inter-relationship between vegetation, topography and burn severity could be exploited as a cost-effective avenue to support future post-fire rehabilitation management and monitoring programmes, such as the one established for Okanagan Mountain Park. Furthermore, we examine the effectiveness of remote sensing technology to provide long-term, continuous monitoring of vegetation recovery dynamics. Thus, the specific objectives were: first to quantify the spatio-temporal patterns of vegetation re-growth dynamics established within the burn scar monitored by the NDVI and RI indices responses; second, to explore potential relationships between vegetation regrowth dynamics and topography properties specific to our study site; third, to investigate the influence of the relationships between vegetation regeneration to burn severity, as expressed by the Differenced Normalized Burn Ratio (dNBR).

## Study area

The Okanagan Mountain Park, British Columbia (B.C.), located in the Montane Cordillera Ecozones of Western Canada at which a fire occurred in 2003 was used as a case study. It is formed as an elbow of pre-quaternary bedrock jutting out from the eastern shore of Okanagan Lake, between the cities of Kelowna and Penticton (Fig. 1). The terrain ranges from examples of undeveloped marine foreshore and semi-desert wilderness at lower elevations to deeply incised melt water channels, rocky outcrops and the 1579 m peak of Okanagan Mountain on the higher elevations (BC Ministry of Environment, 2013). The region is covered mainly by evergreen coniferous forests, predominantly *Pinus ponderosa* and *Pseudotsuga menziesii* species; however grasses and shrubs dominate the lower elevations. The mean elevation is approximately 983 m, while the slopes range from 0 to 89°. The climate of the Okanagan Valley is best described as mild and continental. Summers (traditionally from May to September) are warm and sunny, with average temperatures reaching above 20 °C. The winters (October to February) can range from moderate or temperate, with average temperatures of approximately −3 °C to 2 °C, to cold extremes at the higher elevations (<−10 °C) (Rayne, Forest, & Friesen, 2009). On 16 August 2003 this area experienced catastrophic damage from a wildfire outbreak. The fire began with a lightning strike at a point around 200 m above lake level just south of the City of Kelowna. The fire quickly grew under extremely dry and windy conditions, eventually becoming the most destructive urban/forest interface fire in recent B.C. history, destroying 25,000 ha of forest, forcing the evacuation of more than 27,000 people and destroying 239 homes (BC Ministry of Forest and Change, 2003). Complete destruction of forest vegetation and water-repellant soil conditions were also deemed to be of significant concern due to the elevated risk of flooding should an intense rainfall event occur. Following the fire, a 5 year rehabilitation programme was established which produced a variety of tools to help local governments coordinate and focus additional fire re-vegetation and restoration treatments. This fire event was used in the present study to examine the vegetation regrowth over a period of 8 years (2003–2011) using freely distributed EO data.

## Datasets description

A total of six Landsat TM images (path:45, row:25) were acquired from the United States Geological Survey (USGS) Global Visualization Viewer (<http://glovis.usgs.gov/>). Images were obtained over a period of 8 years covering 2003–2011. Images around

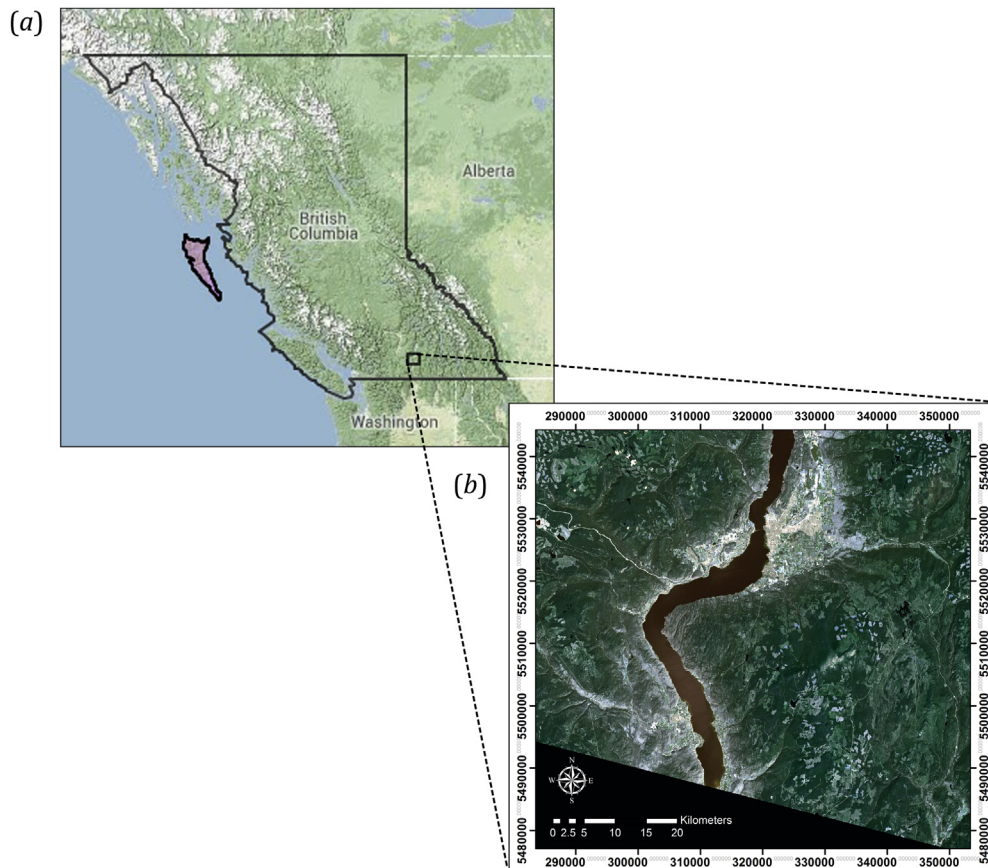


**Fig. 1.** (a) Location of study area within British Columbia, Western Canada. (b) Study area shown here on the subset of the TM image acquired on 17th of July 2003. This is the Okanagan Mountain Provincial Park study area (band combination – 3 RED, 2 GREEN, 1 BLUE). (For interpretation of the references to colour in this figure legend, the reader is referred to the web version of this article).

the same dates of different years were selected to minimise phenological differences, and also circumvent the influence of seasonal differences in both spectral radiation (e.g. Sun elevation angle, Sun–Earth distance, meteorological conditions) and surface reflection. In particular, a TM pre-fire image acquired on 17 July 2003 and five post-fire ones were also obtained on 3 September 2003, 11 September 2006, 14 September 2007, 22 September 2010, and 9 September 2011. All images were acquired geometrically corrected, geometrically resampled, and registered to a geographic map projection with elevation correction applied (Level-1T processing).

In addition, topography information for the study region was obtained from the Advanced Spaceborne Thermal Emission and Reflection Radiometer (ASTER) Global Digital Elevation Model (GDEM). The product version 2 was obtained at no cost from NASA REVERB (<http://reverb.echo.nasa.gov/>). Estimated accuracies of the product are for 20 m at 95% confidence for vertical data and 30 m at 95% confidence for horizontal data (ASTER GDEM, 2009). The dataset is provided in geotiff format, in geographic latitude/longitude projection which uses a 1 arc-second (30 m) grid of elevation postings referenced to the WGS84/EGM96 geoid (Tachikawa, Hato, Kaku, & Iwasaki, 2011).

Lastly, a land cover shapefile (LCC2000-V) was obtained at no cost from the GeoBase website (<http://www.geobase.ca>). This is a federal, provincial and territorial government initiative that is overseen by the Canadian Council of Geomatics (CCOG). Classes in LCC2000-V are based on the combination of Earth Observation for Sustainable Development (EOSD) and the National Land and Water Information Service (NLWIS) of Agriculture and Agri-Food Canada

(AAFC) classifications. The shapefile is a result of the vectorisation of raster thematic data originating from inputting Landsat 5 and Landsat 7 ortho-images and ground reference training data into a Decision-Tree or Supervised image classification process. A detailed description of the retrieval methodology can be found in AAFC (2012) and Wulder et al. (2008). The data was used in identifying the land cover types within the study area and in the geometric correction of the Landsat TM and ASTER GDEM Images.

## Methods

All analysis of the vegetation regeneration for the studied region was carried out using ENVI (v. 5.0, ITT Visual Solutions) and ArcGIS (v. 10.1, ESRI) software platforms. An overview of the steps implemented to satisfy the study objectives is depicted in Fig. 2.

### Pre-processing

All pre-processing was carried out using ENVI (Fig. 2). First, radiometric calibration for each TM image date was implemented. Each spectral band was imported to ENVI and was converted to top of the atmosphere reflectance (TOA) according to the methodology described by Irons (2011). Subsequently, for each image all spectral bands, excluding the thermal infrared (i.e. band 6), were layer stacked to form a single image file corresponding to the acquisition date of each image. Absolute atmospheric correction was then implemented utilising ENVI's atmospheric correction module FLAASH (Fast Line-of-sight Atmospheric Analysis of Spectral Hyperscubes). FLAASH is an atmospheric correction tool that corrects

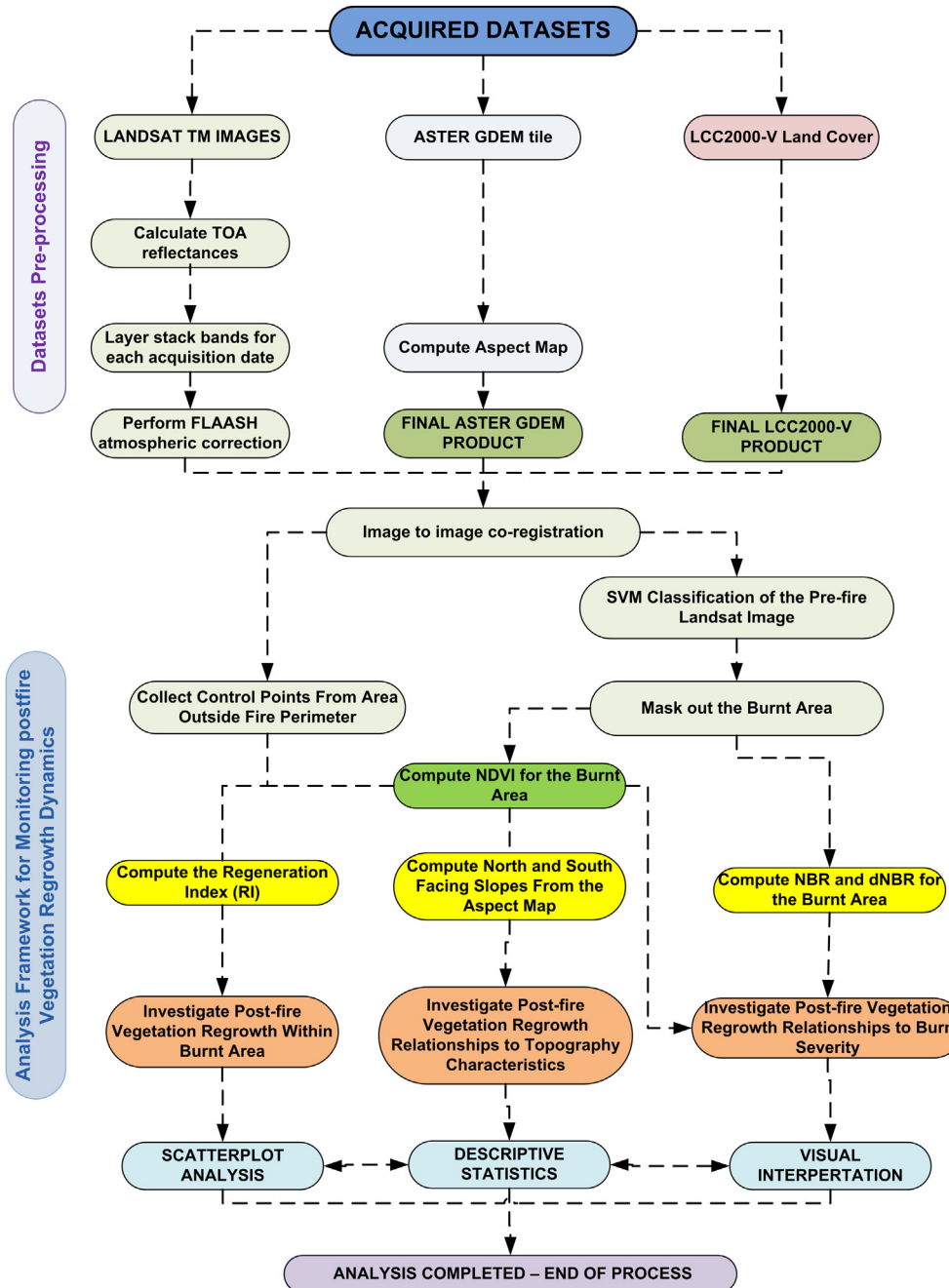


**Fig. 2.** Overall methodology implemented in our study.

wavelengths in the visible through NIR and SWIR regions, up to 3 μm. FLAASH incorporates the MODTRAN4 radiation transfer code (Exelis Visual Information Solutions, 2013). No further topographic correction was necessary as images were already terrain corrected when acquired. All datasets were then co-registered to a common spatial reference frame, since this is a requirement if imagery from different dates is required to be analysed (Schmidt & Glasser, 1998). The Landsat 17 July 2003 pre-fire image was used as a base image to which all other available images were co-registered and projected to the North American Datum 1983 into Canadian Spatial reference System (NAD83CSRS). Image to image registration was performed using twenty five commonly identified Ground Control Points (GCPs) between the different datasets. The nearest neighbour interpolation was employed to resample the image. This resampling method was used to better preserve the digital number (DN)/

reflectance values in the original images. A mean Root Mean Square (RMS) error registration below the TM pixel (30 m) was obtained in all cases that was considered satisfactory.

Delineation of the burnt area was subsequently performed using Support Vector Machines (SVMs, Vapnik, 1995). The motivation of using this machine learning classifier is its intrinsic ability in dealing with non-linear classification problems, while providing tools to easily control over-fitting during the training of the classifier (Petropoulos, Knorr, Scholze, Boschetti, & Karantounias, 2010; Volpi, Petropoulos, & Kanevski, 2013). In addition, implementation of this classifier has also shown promise in burnt area mapping (Petropoulos, Kontoes, & Keramitsoglou, 2011; Petropoulos, Kontoes, & Keramitsoglou, 2012). Here, multi-class SVMs pairwise classification strategy was implemented in ENVI. The classifier was applied at the original spatial resolution of 30 m of the 3

September 2003 post-fire image to derive the burnt area. In defining the SVMs feature space all the sensor reflective bands after the end of pre-processing were used. The Radial Basis Function (RBF) kernel function was used for performing the pair-wise SVMs classification. This kernel was selected as it requires the definition of only a small amount of parameters to run and has also shown generally good results in many classification experiments (e.g. Huang et al., 2008; Petropoulos et al., 2012). RBF kernel was parameterised based on performing a number of trials of parameter combinations, using classification accuracy as a measure of quality. Such an approach has also been adopted in the past in analogous studies of SVMs implementation (e.g. Volpi et al., 2013). The classifier was trained using a random sampling design of points based on the GeoBase land cover shapefile (Exelis Visual Information Solutions, 2013) as well as visual interpretation of the datasets. The area classified as the burn scar was extracted as a vector file (.shp) for integration with the other datasets. Then, the TM images, the ASTER DEM and the land cover map were all layer stacked and subsequently clipped to a smaller area covering an area that included the burn scar and sufficient ample land outside its perimeter. This allowed us to enhance the computational efficiency of the processing that would follow. Next, this dataset was intersected with the burnt area polygon. This last dataset was the one used in analysing the vegetation dynamics occurring within the burn scar area of the Okanagan Mountain Park region. Examples of the final datasets derived upon the pre-processing completion are illustrated in Fig. 3.

#### NDVI computation for the analysis of post-fire vegetation regeneration

A quantification of the vegetation recovery dynamics was performed based on multi-temporal analysis of NDVI (Eq. (1)). This was computed from the R, and NIR spectral bands of each TM image as follows (Rouse et al., 1973):

$$\text{NDVI} = \frac{(\text{NIR} - \text{RED})}{(\text{NIR} + \text{RED})} \quad (1)$$

where NIR and R denote the near-infrared and the red surface spectral reflectance respectively.

NDVI values thus range from  $-1$  to  $+1$ , where zero to negative values correspond to an absence of vegetation (Pettorelli et al., 2005). Thus, NDVI is an expression related to the amount of photosynthetically active vegetation exposed to the sensor within each pixel, and typical NDVI values for vegetated areas are in general well above  $0.1$  (Petropoulos & Kalaitzidis, 2011, chap. 2). This index has a strongly established relationship with change detection in canopy cover and above ground biomass in a wide range of ecosystems (Soudani et al., 2012). Following the NDVI computation, analysis of the regeneration process dynamics was subsequently undertaken. This was done by comparing the pre-fire NDVI spatial pattern to the post-fire patterns of NDVI regeneration. This allowed for the rate and extent of post-fire recovery to pre-fire levels to be determined. A series of descriptive statistics of the NDVI within the burn scar were computed from each TM image. Those together with visual, scatterplot and non-parametric correlation analysis (e.g. Hope, Tague, & Clark, 2007; Petropoulos et al., 2014) were used to evaluate the spatial and temporal NDVI regeneration dynamics within the burn scar area.

#### Post-fire vegetation regeneration based on Regeneration Index (RI)

Further analysis was undertaken to quantify the vegetation regrowth dynamics of the study site on the basis of the Regeneration Index (RI, Díaz-Delgado et al., 1998; Riaño, Chuvieco, Salas, et al., 2002; Riaño, Chuvieco, Ustin, et al., 2002). For its computation, NDVI values between burned plots are compared to those unburned control plots within the same image that contained spectral and environmental characteristics similar to the state of the pre-fire burn scar area (Díaz-Delgado et al., 1998; Lhermitte, 2007). The mean NDVI value of the fire area is subsequently calculated and divided by the calculated mean NDVI value of the control plots using the following formula:

$$\text{RINDVI} = \text{NDVI}_{\text{fire}} / \text{NDVI}_{\text{control}} \quad (2)$$

where  $\text{VI}_{\text{fire}}$  is a measure of the vigour of the vegetation (NDVI) for a burned plot and  $\text{VI}_{\text{control}}$  is the NDVI for an unburned control plot. RI

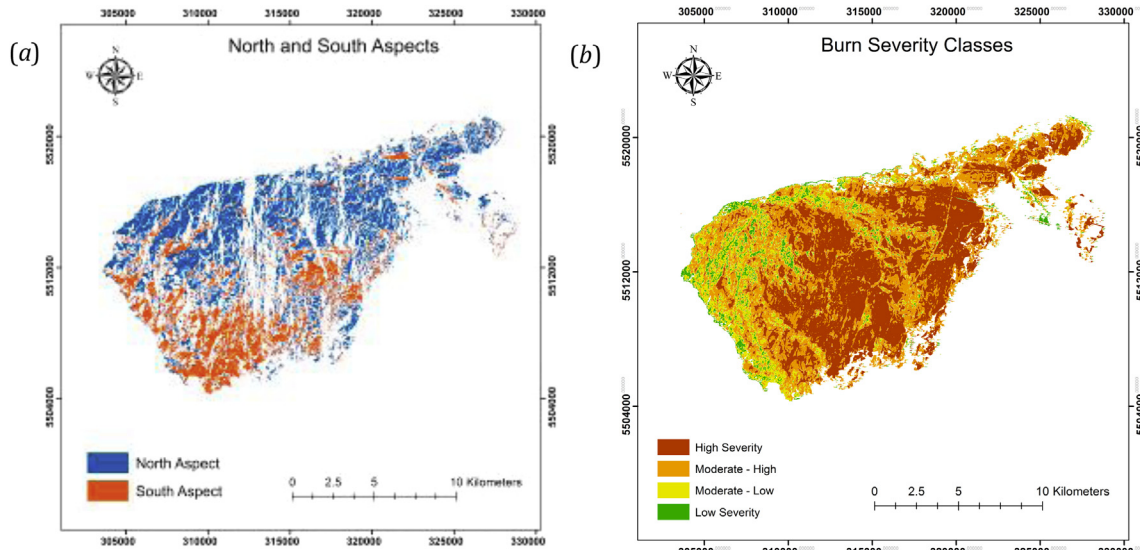


**Fig. 3.** (a) Northern and Southern aspects of the area covered by the burnt area envelop, derived from ASTER Global Digital Elevation (GDEM) product upon completion of the pre-processing steps, (b) Burn severity map showing the spatial extent of each level of burn severity class within the burn scar.

provides values from 0–1 (values are indicative of percentage of recovery e.g. 1 equals 100% recovery to pre-fire levels). As analysis of NDVI rates independently can cause the development of false trends in the data due to a wide range of noise factors that reduce the detection of regeneration patterns (e.g. interannual or micro-climatic differences), this index essentially standardises multi-temporal measures of NDVI between the different EO images used based on these control points. Thus, variations of RI are interpreted to be solely due to the regeneration process and to be independent of spectral differences between image dates caused by other effects (Riaño, Chuvieco, Salas, et al., 2002; Riaño, Chuvieco, Ustin, et al., 2002).

In our study, four separate control plots (CA) were located for each fire area using the 17 July 2003 pre-fire image. Due to the large size of the fire area, multiple control plot polygons were required in order to fully capture the variability exhibited in the pre-fire conditions. Four control plots were chosen to calculate the burn scar area RI values (Fig. 4). Control plots 1 (CA 1) and 2 (CA 2) were chosen based on the specifications described by Díaz-Delgado et al. (1998) and Riaño et al. (2001) as they shared similar spectral and environmental conditions to the pre-fire burn scar area. Control plots 3 (CA 3) and 4 (CA 4) were chosen based on their differing characteristics. CA 3 was based in an environment consisting of a

majority of dense coniferous forest which had consistently higher NDVI values compared to the pre-fire burn scar area, and CA 4 was based in an agricultural environment affected by anthropogenic activity and livestock grazing. These control plots were selected to evaluate the effectiveness of accurate control plot selection on RI values, and to analyse how selection of areas that are spectrally and environmentally different to pre-fire levels affect RI trends and values. The mean NDVI values from all these plots were subsequently extracted and compared between the pre-fire and all post-fire TM images. A series of statistical parameters were then computed which allowed for the determination of the extent to which the pre-fire pattern was re-established, and the rate of this recovery within the burn scar.

#### Topography analysis

The relationship between vegetation recovery dynamics and topography, in particular aspect were investigated. Aspect analysis was conducted in ArcGIS using the aspect map produced from the ASTER GDEM previously acquired. In accordance to previous studies (Fox et al., 2008; Petropoulos et al., 2014; Wittenberg et al., 2007), pixels with an orientation between NW (315°) and NE (45°) were classified as north facing slopes, whereas as south facing

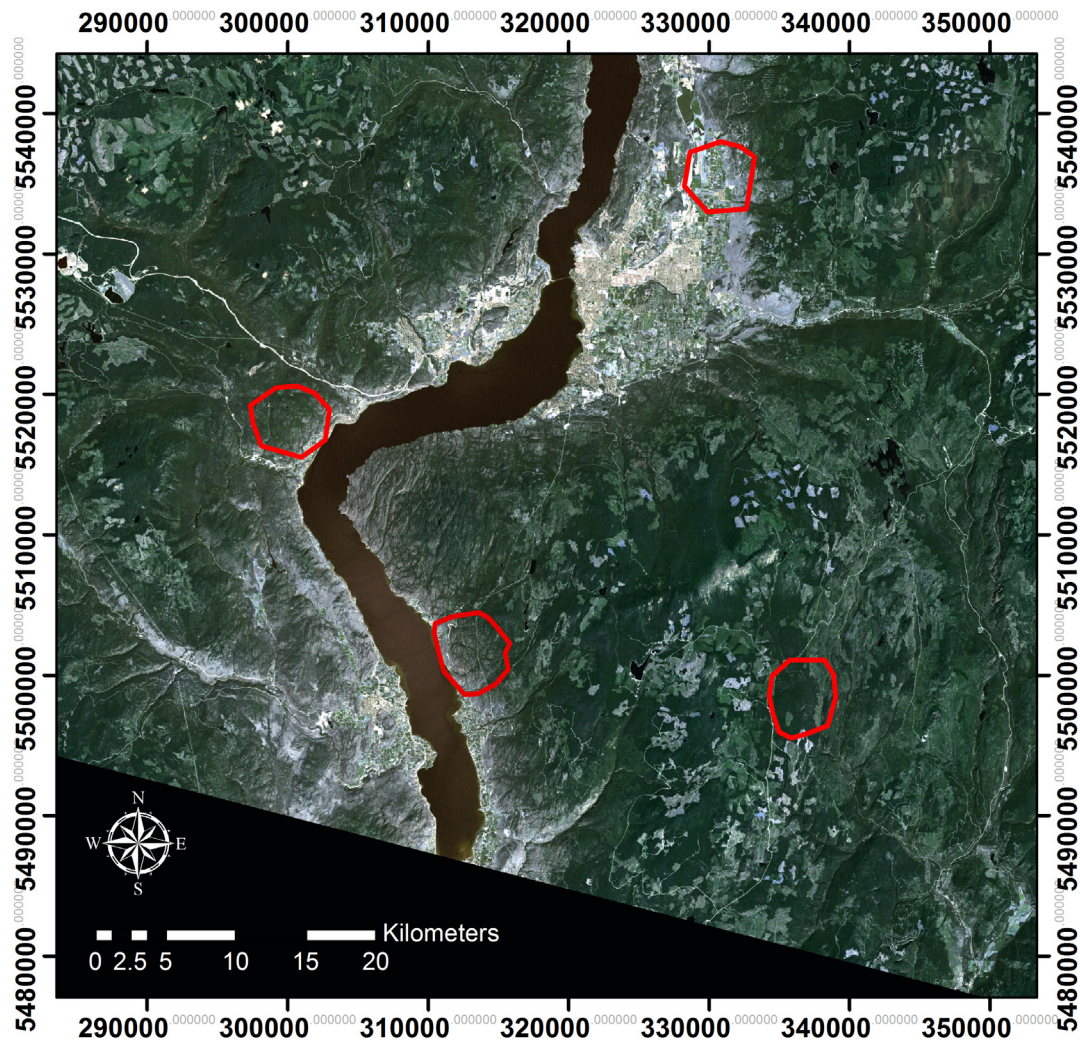


**Fig. 4.** The four control areas (CA) chosen to calculate the burn scar RI values. CA 1 and 2 (similar spectral/environmental conditions to pre-fire burn scar area), 3 (Forest) and 4 (Agricultural).

slopes were classified as those that had an orientation between SE ( $135^\circ$ ) and SW ( $225^\circ$ ). Pixels within the burn scar not falling within these value ranges were excluded from this type of analysis. All relevant statistical analyses were performed using SPSS v. 18 software package (SPSS Inc., Chicago, IL).

### Burn severity mapping

Burn severity was mapped utilising the Normalized Burn Ratio (Eq. (3)) (NBR), an index defined to highlight areas that have been burned and to indicate the severity of the burns (Key & Benson, 2005). NBR utilises the differing responses of Landsat bands 4 (NIR,  $0.76\text{--}0.90\ \mu\text{m}$ ) and 6 (SWIR,  $2.08\text{--}2.35\ \mu\text{m}$ ) which are sensitive to changes in soil and vegetation moisture (Garcia & Caselles, 1991) and is computed as:

$$\text{NBR} = \frac{\text{NIR} - \text{SWIR}}{\text{NIR} + \text{SWIR}} \quad (3)$$

Often, the NBR is calculated for both pre-fire and post-fire satellite scenes, and then the two pre-/post-fire ratios are differenced (dNBR) to generate a scaled index of burn severity, the Differenced Normalised Burn Ratio (Eq. (4), dNBR; Key & Benson, 2005).

$$\text{dNBR} = \text{NBR}_{\text{pre}} - \text{NBR}_{\text{post}} \quad (4)$$

The application of the dNBR to Landsat imagery has shown to be an effective method to map burn severity within temperate forests (Cocke, Fulé, & Crouse, 2005; Van Wagendonk et al., 2004) and boreal forests (Epting, Verbyla, & Sorbel, 2005).

Herein, the NBR was calculated for both pre-fire and post-fire satellite scenes, before the pre/post fire ratios were differenced to generate a scaled index of burn severity. The index was based on values derived from the USGS FIREMON program (USGS, 2004) shown in Table 1. Generally, unburned areas (i.e. no change between pre and post-dates) have dNBR values near zero; whereas the higher positive values are connected to the more severely burned areas (i.e. fire changed them the most). It is possible to have dNBR values less than  $-0.550$  or greater than  $1.350$ , but usually these are not considered burned, rather, they are likely anomalies caused by miss-registration, clouds, or other factors not related to real land cover differences (USGS, 2007). Descriptive statistics of NDVI within each level of burn severity were subsequently computed from each TM image, together with scatterplot and non-parametric correlation analysis to evaluate the effect of burn severity on vegetation regeneration and produce thematic maps of burn severity.

## Results

### Quantifying vegetation regeneration dynamics

The NDVI and RI results for the different days and the corresponding descriptive statistics for the burn scar area are depicted in Tables 2–4. Furthermore, the NDVI maps computed for the area

**Table 2**

Changes in NDVI for the area under the burn scar during the study period.

Landsat TM image date	Minimum NDVI	Maximum NDVI	Mean NDVI	NDVI Standard Deviation
July 2003 (Pre-Fire)	-0.125	0.887	0.652	0.133
August 2003	-0.145	0.881	0.266	0.135
September 2006	-0.099	0.879	0.406	0.098
September 2007	-0.117	0.872	0.431	0.127
September 2010	-0.117	0.886	0.462	0.125
September 2011	-0.138	0.887	0.463	0.131

**Table 3**

Results of the regression analysis of scatterplot data, examining vegetation regrowth dynamics in all post-fire image dates in relation to the pre-fire conditions.

Period	Slope	Intercept	R <sup>2</sup>
July 2003 (Pre-Fire) – August 2003	0.108	0.624	0.012
July 2003 (Pre-Fire) – September 2006	0.475	0.100	0.412
July 2003 (Pre-Fire) – September 2007	0.720	0.342	0.472
July 2003 (Pre-Fire) – September 2010	0.726	0.325	0.524
July 2003 (Pre-Fire) – September 2011	0.746	0.307	0.541

under the burn scar for each TM image date are also shown (Fig. 5). Fig. 6 displays the NDVI difference maps produced from the comparison of pre- and post-fire NDVI.

Visual interpretation of the pre- and post-fire NDVI and NDVI change maps showed an abrupt decrease in NDVI following the fire followed by an increase in NDVI in subsequent years. Comparison of the pre- and post-fire mean NDVI images clearly showed that the majority (>50%) of the pre-fire image contained values above  $\sim 0.4$  (suggesting dense green biomass). However, there has been a large decrease in mean NDVI values in the immediate post-fire image, with a majority (>50%) of the image consisting of values below 0.3 (Fig. 5). This is further supported by the pre- and post-fire NDVI difference map (Fig. 6) where over 35% of the burn scar area had a maximum decrease of 0.762 in mean NDVI between both images and additionally over 75% of the entire area is showing an overall decrease in mean NDVI from pre-fire levels. The NDVI difference maps also demonstrated a general trend of gradual regeneration from the initial post-fire change map to the final year difference map (September 2003 post-fire – September 2011). This is combined with an increase in the overall spatial extent of positive recovery in mean NDVI (Fig. 6). As can also be observed, stronger regrowth dynamics appear to occur in the East of the burn scar area compared with low growth in the West, whereas the North and South areas show moderate regrowth.

Regression models were fitted to the dynamics of the regeneration process in agreement to other studies (e.g., Hope et al., 2007; Petropoulos et al., 2014), where the relationship between pre-fire burn scar area NDVI pixel values against subsequent post-fire dates were plotted in a series of scatterplots (Fig. 7). The location

**Table 1**

The scaled index of burn severity based on values derived from the USGS FIREMON program (USGS, 2007).

dNBR	Burn severity class
<-0.25	High post-fire regrowth
-0.25 to -0.10	Low post-fire regrowth
-0.10 to +0.10	Unburned
0.10 to 0.27	Low-severity burn
0.27 to 0.44	Moderate-low severity burn
0.44 to 0.66	Moderate-high severity burn
>0.66	High-severity burn

**Table 4**

Mean RI values for the 4 control areas for each image date.

Year	Mean RI			
	Control area 1	Control area 2	Control area 3	Control area 4
July 2003 (Pre-Fire)	1.012	1.024	0.929	1.186
August 2003	0.386	0.396	0.357	0.487
September 2006	0.622	0.625	0.570	0.649
September 2007	0.666	0.676	0.609	0.673
September 2010	0.724	0.719	0.659	0.815
September 2011	0.726	0.721	0.661	0.837

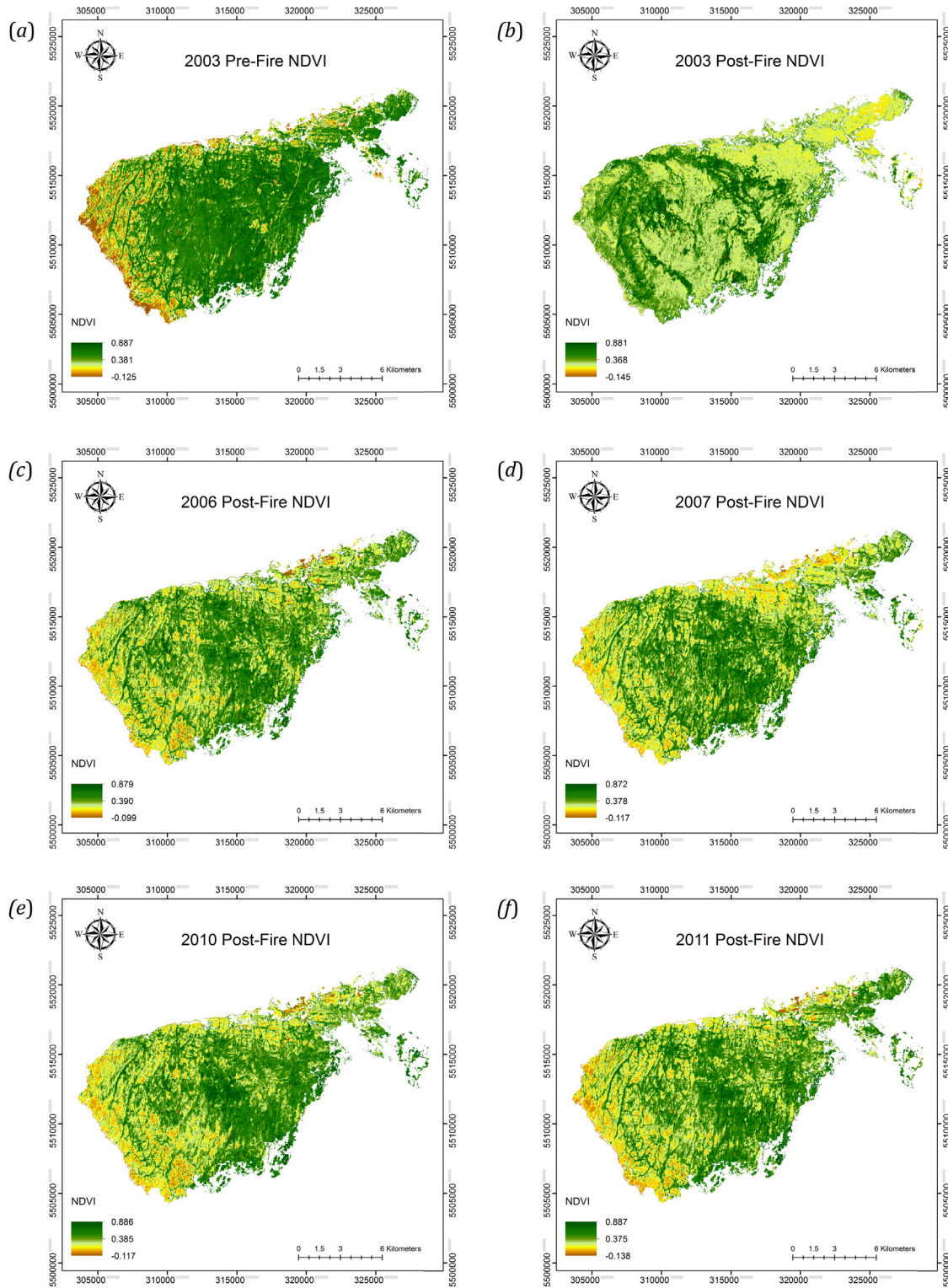


**Fig. 5.** NDVI maps computed from our pre-processed Landsat TM images: (a) July 17th, 2003, (b) September 3rd, 2003, (c) September 11th, 2006, (d) September 14th, 2007, (e) September 22nd, 2010, and (f) September 9th, 2011. The initial decrease in the mean NDVI following the fire and the gradual regeneration over time is evident.

of the cloud of points relative to the 1:1 line represents the return of the entire burn scar area to pre-fire NDVI conditions, while the degree of coherence in the pre- and post-fire NDVI spatial patterns for each year is represented by the scatter of points. Slope, intercept and  $R^2$  statistics (coefficient of determination) for the regression line plotted through the data were calculated (Table 3). As can be

observed from Fig. 7, the movement of the regression line back towards the 1:1 line and the increase of the  $R^2$  values with time was very gradual. Also, for the entire burn scar, NDVI had only returned to ~55% (0.542) of the pre-fire level after 8 years (Table 3). Notably, highest increase in  $R^2$  was found during the initial 3 year period following the fire with a more gradual return in subsequent years,

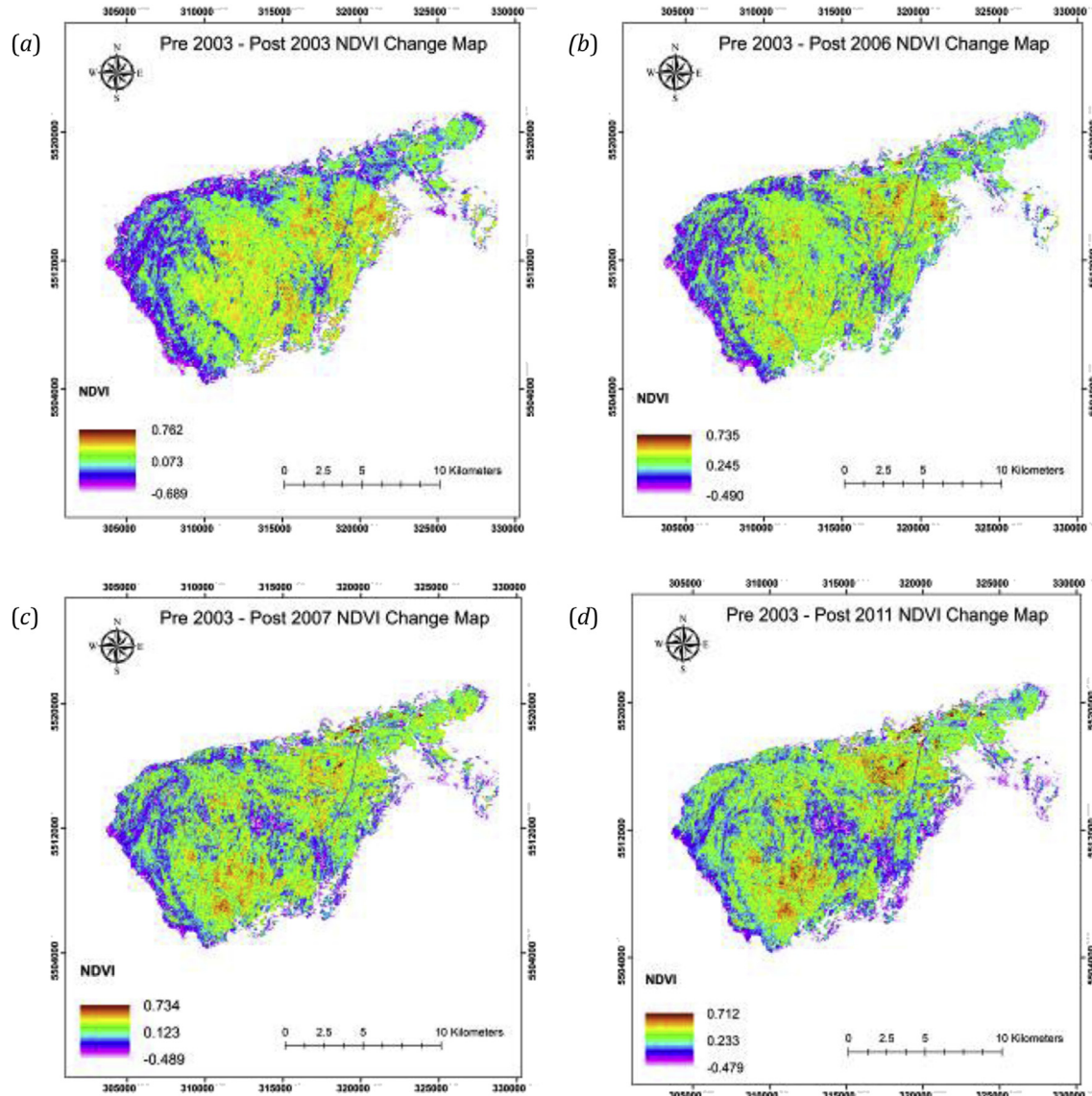


**Fig. 6.** Examples of NDVI difference maps for the area under the burn scar, (a) between the 2003 pre- and 2003 post-fire images and between the 2003 post-fire image and (b) 2006 (c) 2010 and (d) 2011 post-fire images. 2003 Pre-2010.

where there was an increase of 0.400 in  $R^2$  by 2006 compared to only an increase of 0.129 for the subsequent 5 years.

Multi-temporal RI results for the four control plots were compiled in Table 4 and Fig. 8 to facilitate further analysis. Pre-fire RI values evidently varied between the 4 control plots. Control plots 1 and 2 had RI pre-fire values nearing 1, indicating that the control plots shared similar pre-fire condition to that of the burn scar area (CA 1 = 1.012, CA 2 = 1.024). However the remaining control plots showed pre-fire RI values ranging from above 1.186 to below 0.929, indicating differing characteristics (Table 4). Over the 8-year period, RI values of control plots 1 and 2 indicated a gradual trend toward green biomass recovery as seen in Table 4 and Fig. 8. The RI values obtained suggest a return to over ~70% of the NDVI pre-fire levels by 2011 which correlates strongly with the NDVI regeneration dynamics. These results emphasise the importance and effectiveness of the RI either as an alternative, or complimentary to the NDVI trend analysis performed previously.

A comparison of the spatial extents of the vegetation regeneration with the land cover types of the GeoBase Land Cover Shapefile

suggests that pre-fire land cover type has an effect on recovery rates. Indeed, areas dominated by herbaceous and shrub land cover types as identified in the GeoBase Land Cover, returned to near pre-fire levels within the time period of this study. Nevertheless, areas composed of mainly woodland, displayed more gradual rates of regeneration and could take decades to revert to pre-fire levels.

#### Vegetation regrowth and topography

The results associated with the examination of the relationships between vegetation regrowth and topography are presented in Table 5 and Fig. 9. Table 5 summarises the descriptive statistics for the NDVI across the whole area under the burn scar for the north- and south-facing slopes separately. Both aspects showed an abrupt decreased in mean NDVI immediately after the fire in both the north and south respectively, with a gradual trend back towards pre-fire levels in all subsequent image dates. Regeneration appeared to be faster on north-facing slopes in comparison to south-facing slopes. Indeed, for example, mean NDVI on north-

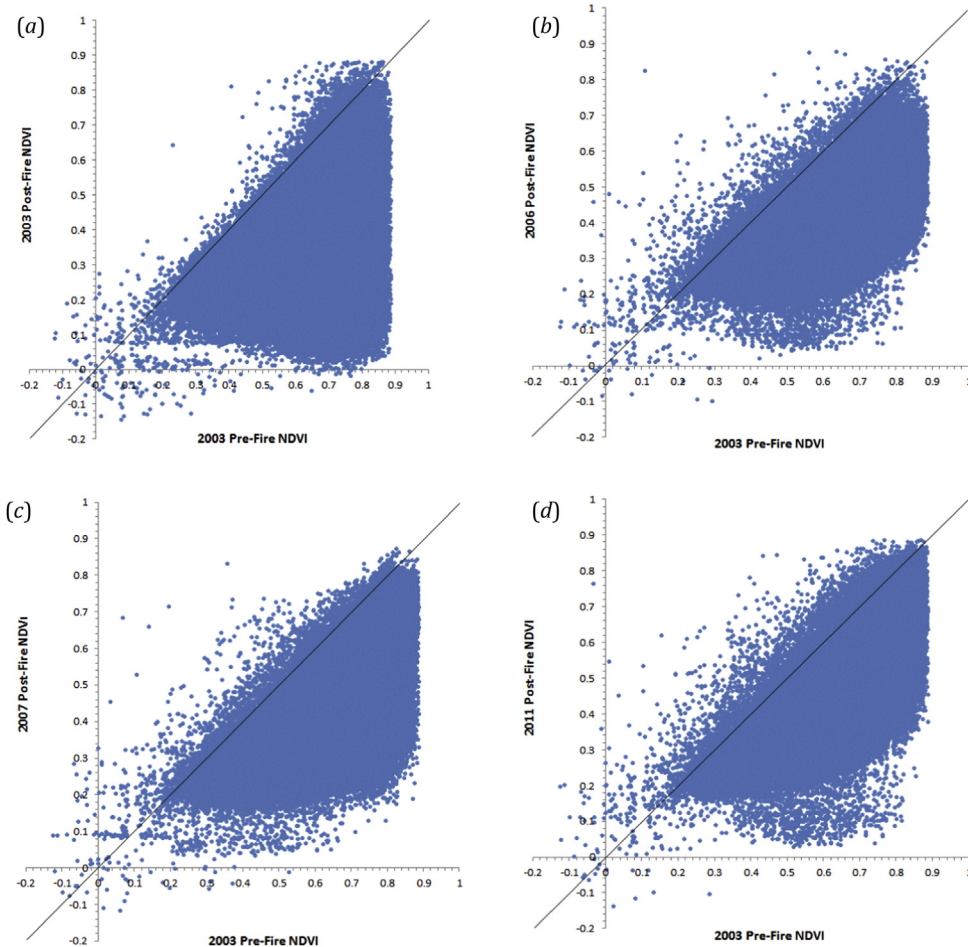


**Fig. 7.** Examples of scatterplots of pre-fire NDVI (July 17th 2003) against post-fire (a) September 3rd 2003 (b) September 11th, 2006 (c) September 14th 2007, and (d) September 9th 2011. It can be observed the gradual increase of the slope to pre-fire conditions, which is suggesting regrowth in the area.

facing slopes increased from 0.256 to 0.422 between September 2003 and September 2006 and then to 0.482 in September 2011, showing an initial rapid increase followed by a more gradual return in the latter 5 year period. On south facing slopes the increase appeared lower, from 0.272 to 0.377 between September 2003 and September 2006 and then to 0.427 in September 2011.

There are observable similarities between the regeneration trends of the overall burn scar and both aspects. The mean NDVI values exhibited a gradual return to pre-fire levels with both northern and southern exposures only returning to ~71% and ~70% of pre-fire levels respectively. Similarly to the overall burn scar statistics, mean NDVI values showed that the largest increase in

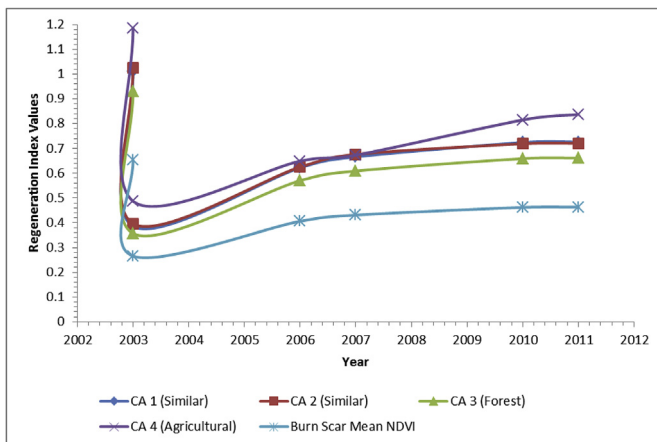


**Fig. 8.** The regeneration index values associated with each control point for each image date.

**Table 5**

NDVI changes for the area under the burn scar, separately for: (a): north facing, and, (b) south facing slopes.

Landsat TM Image date	Minimum NDVI	Maximum NDVI	Mean NDVI	NDVI Standard deviation
<i>(a) North facing slopes only</i>				
July 2003 (Pre-Fire)	-0.066	0.887	0.675	0.120
August 2003	-0.133	0.880	0.256	0.138
September 2006	-0.095	0.877	0.422	0.095
September 2007	-0.109	0.872	0.440	0.126
September 2010	-0.114	0.886	0.482	0.122
September 2011	-0.050	0.882	0.483	0.127
<i>(b) South facing slopes only</i>				
July 2003 (Pre-Fire)	-0.032	0.887	0.614	0.146
August 2003	-0.126	0.881	0.272	0.125
September 2006	-0.013	0.845	0.377	0.097
September 2007	-0.090	0.865	0.412	0.128
September 2010	-0.117	0.876	0.422	0.122
September 2011	-0.103	0.885	0.427	0.132

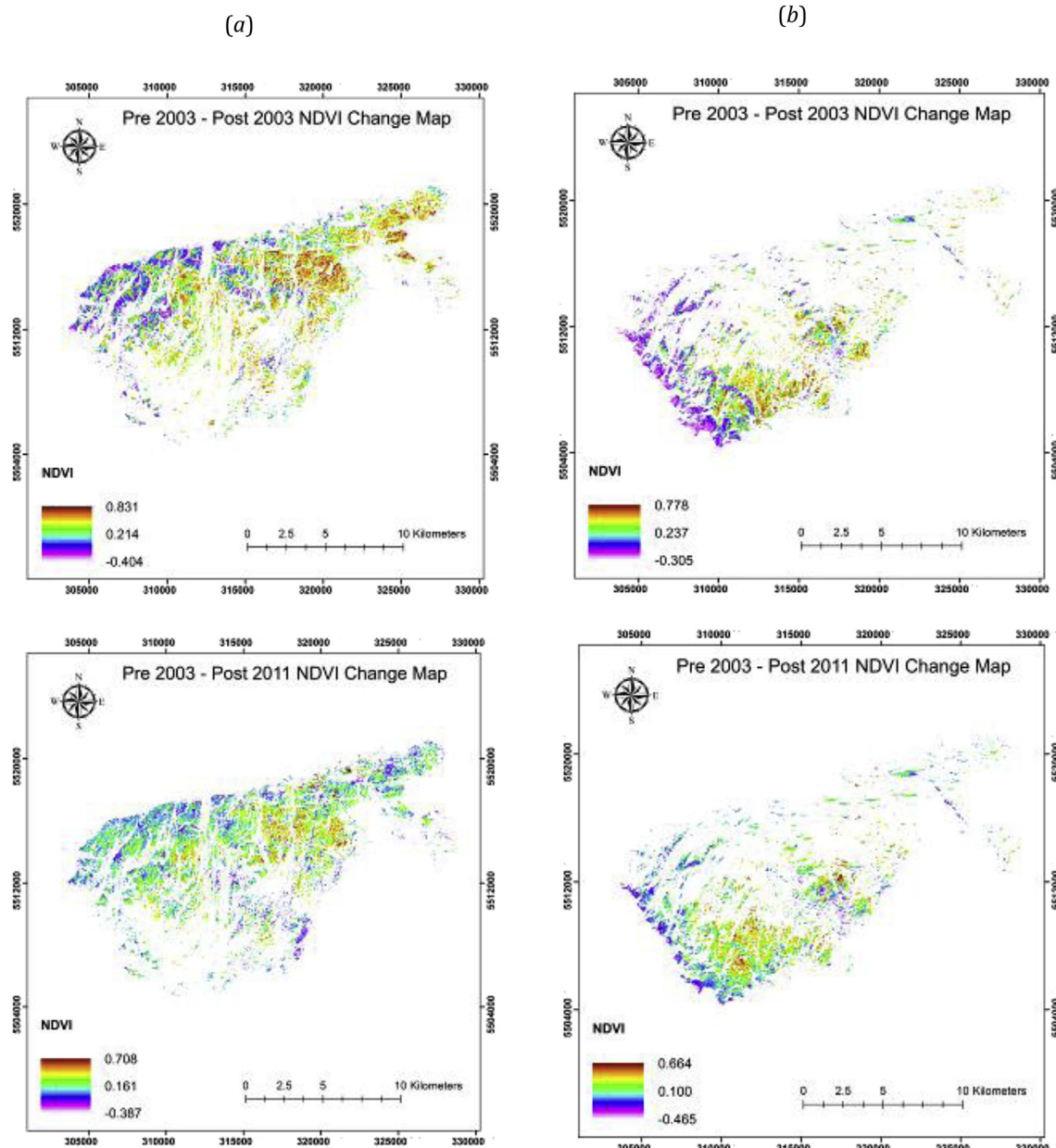


Fig. 9. Examples of NDVI difference maps for northern (a) and southern aspects (b).

regeneration rates was for the 3 year period following the fire, with an increase of 0.166 in mean NDVI in northern aspects and 0.105 in southern aspects, compared to an increase of only 0.060 and 0.050 in the subsequent 5 years.

#### Vegetation regrowth and burn severity

Burn severity was examined utilising the NBR and dNBR indices to produce a burn severity map which was used in comparison with vegetation regeneration data. Table 6 and Fig. 3b illustrate the results associated with the examination of the relationships between vegetation regrowth and burn severity. As can be observed in Fig. 3b, the majority of the burn scar area experienced high severity burns (41.2%), followed by moderate to high (37.1%). There was only a very small percentage of the area that experienced low levels of burn severity (9.3%). Table 6 describes the results of the mean NDVI

values located within each level of burn severity. As was perhaps expected, the largest change in mean NDVI was within areas of high severity burn, where mean NDVI values decreased by 0.537, from 0.734 in July 2003 to 0.197 in September 2003, 18 days after the fire. This was followed by areas of moderate to high severity burns which decreased by 0.331 over the same period. The areas of low burn severity only experienced a decrease of 0.306 in mean NDVI values, less than 25% of the decrease that was recorded within the areas of high severity burn. After the initial 3-year recovery period, the higher regrowth is located within areas of low severity burns (Table 6), where mean NDVI has returned to 64% of pre fire mean NDVI levels compared to only 58% in the areas of high burn severity. This trend is continued in the remaining 5 years of the study period where areas of low severity burns have returned to 72% of pre fire levels by 2011 compared to only 70% in the areas of high severity burns.

**Table 6**

Relationship between vegetation regeneration dynamics as expressed from the mean NDVI within areas of Low Severity, Low to Moderate, Moderate to High and High Severity burn classes (derived from the dNBR) are summarised.

Year	Mean NDVI within classes of burn severity			
	Low severity	Low to moderate	Moderate to high	High severity
July 2003 (Pre-Fire)	0.611	0.519	0.625	0.734
August 2003	0.305	0.359	0.294	0.197
September 2006	0.394	0.388k	0.391	0.424
September 2007	0.413	0.389	0.414	0.462
September 2010	0.436	0.415	0.433	0.509
September 2011	0.437	0.427	0.441	0.517

## Discussion

### Post-fire vegetation regeneration

Results of this study showed that fire is a significant agent of change within the Montane Cordillera Ecozone of our study area. The abrupt decrease in NDVI values immediately following the fire is evidence of these effects. Main findings also suggest that vegetation regeneration can potentially take decades to revert to a pre-fire state in such ecosystems as exhibited in the interior Douglas-fir and Ponderosa pine zones of our study area. Indeed, eight years after the fire, NDVI levels had only returned to ~60% of pre-fire levels and the spatial extent of vegetation had not reverted to its original state. In contrast, succession of a burned site in more mature boreal ecosystem of more northerly latitudes may take 50–200 years before it has reverted to pre-fire levels. However, these types of ecosystems have experienced a decrease in the frequency of annual fire events where frequent stand-replacing fires have not been the norm, thus allowing tree stands to mature for decades or even centuries (Wallenius, Pitkänen, Kuuluvainen, Pennanen, & Karttunen, 2005). Vegetation regeneration rates in warmer climates such as Mediterranean ecosystems are generally much shorter (Arianoutsou et al., 2010).

The highest regeneration rates in the study area were observed during the 3-year period following the fire, and this trend was evident throughout the study reflecting the rapid regrowth of vegetation immediately following the fire. This is especially true of the bunch grass zones of the study area, which consist of grasslands dominated by bunch grass, herbaceous vegetation and shrub species (BC Ministry of Forest and Change, 2003). This is due to the little above-ground structural tissue of these species type, and so almost all new tissue fixes carbon and contributes to growth (D'Antonio and Vitousek, 1992). Analysis of the pre-fire land cover suggests that the largest area of coniferous species (*P. ponderosa*, *P. menziesii*, *Pinus contorta* and *Picea engelmannii*) was located within regions of high severity burn. Benson and Green (1987) suggest this is due to the advent of aggressive fire suppression which has resulted in an increased encroachment of shade-tolerant *P. menziesii* within the understory of the *P. ponderosa* stands. When fire occurs in these mixed forests, the understory *P. menziesii* act as a fire ladder making crown fires much more likely, and these fires result in complete destruction of stands of all ages. As these species typically reach reproductive maturity at 12–15 years. If post-fire management of these areas is inadequate there is a possibility for invasive non-native species as well grasslands to occupy the burnt area and compete for the fertile ground (Arno, Harrington, Fiedler, & Carlson, 1995). However, the continued gradual increase in mean NDVI which follows the initial post-fire regeneration, accompanied by the high mean NDVI values, suggest that tree stands have re-established in the area (Maxwell, Airola, & Nuckols, 2010).

Ground surveying or very high resolution satellites could help validate these results for a more accurate overview. More gradual vegetation regrowth during subsequent periods also suggests improvement in the soil and hydrological characteristics of the region as they return to a pre-fire state.

The results of the RI showed a strong correlation between RI values and mean NDVI. It should be noted that both indices followed similar trends, suggesting gradual regeneration rates and return to pre-fire levels. Overall, the RI index was determined to be largely independent of radiometric calibration uncertainty, minor errors in the atmospheric correction, and differences in the phenological state of the vegetation (Riaño, Chuvieco, Salas, et al., 2002; Riaño, Chuvieco, Ustin, et al., 2002). Control plots 1 and 2 were selected for their spectral and environmentally similar characteristics to the pre-fire burn scar area, and had pre-fire RI values of ~1, indicating near identical characteristics. Although stable RI values approaching a value of 1 would indicate recovery, as discussed earlier, forest stands that have been removed by catastrophic crown fires may take decades to regenerate to their pre-fire state and thus full recovery was not expected in many areas of the study site (Graham, McCaffrey, & Jain, 2004). The necessity for accurate selection of control plots was very important in the successful use and interpretation of RI. To emphasise this, in this study control plots 3 and 4 were based upon ecosystems with differing characteristics to the burn scar area (forested and agricultural ecosystems respectively). The forested (CA 3) ecosystems exhibited higher NDVI values, and subsequently lower RI values, due to its greater amount of green biomass. The inconsistent values associated with the agricultural ecosystem (CA 4) could possibly be attributed to the anthropogenic influence on NDVI values, associated with crop cultivation and grazing. As a result, frequently updated species, structure and composition data could be used to characterise the increasing and stabilising NDVI and RI values within fire areas over time (Quayle, Brewer, & Williams, 2005).

### Vegetation regeneration and topography

NDVI multi-temporal analysis statistics and also regression models fitted to the data analysed in this study showed that north facing aspects exhibit higher rates of vegetation regeneration compared to south facing exposures. This is in common with other studies conducted within the northern hemisphere (e.g. Cerdà and Doerr, 2005; Fox et al. 2008; Wittenberg et al. 2007). It is clear that aspect is a key control on the rate of vegetation regeneration and reflects the local effects of microclimate on hydrological processes, which are key in triggering vegetation re-growth. Such differences in post-fire regeneration can both reflect and influence localised hydrological variability and soil hydrophobicity, which without proper management can lead to hazardous secondary fire effects (Cerdà and Doerr, 2005). Increased runoff, flooding, debris flows, changes in overland flow patterns and soil erosion (due to the altering of physical and chemical soil attributes and the removal of ground cover and protective vegetation), as well as litter on the forest floor are all major secondary fire effects that can cause further detriment to an already damaged ecosystem (Shakesby & Doerr, 2006; Stewart, Radeloff, & Hammer, 2003). Generally precipitation events are an important factor within vegetation regeneration dynamics; however after a fire event they can be of high concern. This is due to the indirect effect fire has on changes in local hydrological systems, especially in high intensity summer thundershowers, which can pose great risks to erosion rates and even cause landslides (Cannon, Gartner, Wilson, Bowers, & Laber, 2008). Furthermore nutrient losses to streamwater, groundwater, and the atmosphere are also enhanced following fire, significantly affecting

the chemistry of the atmosphere regionally and globally (Crutzen & Andreae, 1990).

#### Vegetation regeneration and burn severity

The spatial extent of the pre-fire vegetation was concentrated on the south-eastern side of the burn scar. These areas were predominantly coniferous forests and grasslands on shallow slopes. The concentration of dark green regions (indicating higher NDVI) in the July 2003 image date (Fig. 5) was centred on this area, indicating healthier more photosynthetically active vegetation cover was present. During analysis of regeneration in the subsequent image dates we can see that the greatest regeneration is also more prominent in this area (Fig. 5). This is supported by the green and blue areas in Fig. 6 (indicating greater regeneration) in the difference maps that indicate that vegetation regeneration was focused to a greater extent on these areas. These factors point to a spatial heterogeneity in vegetation and landscape response as a result of more localised factors. This more complex pattern of vegetation regeneration is also in good agreement with many studies (e.g. Turner et al. 1997).

The results of the burn severity correlated well with the NDVI values of the post-fire image date, where the majority of high severity burn areas overlapped with areas of greatest NDVI decrease. This in line with several studies (e.g. Miller and Yool 2002). Our results suggested that the upland areas (higher elevation) contained a higher percentage of forest cover. These areas experienced a greater initial drop in mean NDVI values while also displaying the lowest vegetation recovery rates in relation to pre-fire mean NDVI values. This is most likely related to the greater amount of pre-fire biomass in the forested areas which would have encountered higher intensity fires. Furthermore, the composition of the forested areas comprise of mainly *P. ponderosa*, *P. menziesii*, *P. contorta* and *P. engelmannii*, which as discussed earlier can require years to recover after fire. This explains the lower relative recovery values exhibited in these areas, compared to areas of grass, shrubs and herbs. An analysis of the burn severity pattern using dNBR also found forested land cover types tended to experience a greater percentage of higher burn severity compared to herbaceous and shrub types. The results of this study support the strong correlation between both indices (Duffy, Epting, Graham, Rupp, & McGuire, 2007). Application of dNBR to Landsat imagery has shown to be an effective method to map burn severity within ecosystems similar to our study area (Cocke et al. 2005; Van Wagendonk et al. 2004) and also regions in more northern latitudes (Epting et al. 2005). Yet, dNBR has been found to often saturate burn severity results (Murphy, Reynolds, & Koltun, 2008) thus not fully capturing the differences in large areas of heterogeneous burn severity seen among larger fires. This was evident in our burn severity map where a large area of heterogeneous high severity burn dominated the burn scar area. In addition, while larger fires do tend to have larger areas of high burn severity they also display more within-fire burn severity variation (Murphy et al., 2008). A single mean dNBR may not reflect the variations within the levels of burn severity of a larger fire as accurately as it would for a small fire. For instance, the burn severity distribution of our fire was ~9% low, 16.6% low, ~12% low-moderate, ~37% moderate-high and 41% high. Since the fire was ~78% moderate/high burn severity, dNBR was likely limited in explaining a majority of the variation in the more severe areas of burn severity. Ultimately the results of this study and current literature suggest that this index is very promising for future fire impact research within these ecosystems.

Hemiboreal or montane ecosystems consist of similar biogeoclimatic zones to those that dominate our study site, predominantly the Interior Douglas-fir and Ponderosa pine zones, and

recovery of these ecosystems can be heavily dependent on the type of fire and extent of damage and mortality rates that accompany it (Jayen, Leduc, & Bergeron, 2006; Marozas, Plausinyte, Augustaitis, & Kaciulyte, 2011). Low to moderate fires in both zones are an integral part of each species fire regimes however higher severity burns can be deleterious for these regions. In the case of the Ponderosa pine and Interior Douglas-fir zones, such fire severities can cause landscape-scale tree mortality, severe soil damage, loss of seed sources, establishment of invasive species and damage to critical wildlife habitat. The implications of this for the long term sustainability of these types of ecosystems in a future of more frequent and severe fires are significant. Since these forests may not be allowed the time to develop into stable communities that are able to recover quickly, the resilience of these ecosystems will therefore be significantly reduced under a regime of increased fire frequency and severity (Díaz-Delgado et al. 2002).

Results provided from the study have shown the promising potential of remote sensing as a cost-effective support structure for current post-fire rehabilitation programmes. Analysis of the spatial distribution of the higher severity burn areas, and their correspondence with vegetation type and topography, could assist planners and managers in recognising areas which might need semi-regular stand maintenance treatments to reduce ground fuel build-up, keep understory regeneration and ladder fuel development in check, and open grown tree pruning to reduce the potential for fire migration from the ground to forest crown. Such areas could also be viable options for cattle grazing to reduce the amount of understory grass and its associated fire hazard (though cattle management plans would have to consider the protection of riparian areas and the general lack of water in the area), or areas suitable for fire prevention engineering techniques (firelines, contingency firelines, backburning and wetting unburnt fuels, control lines, boundaries or breaks that contain no combustible material). Furthermore, remote sensing is able to provide long-term synoptic, repeatable views of fire affected regions in a cost-effective manner. It is vitally important to monitor the long-term post-fire trends in burned areas, which can be a difficult task without the use of remote sensing technology due to logistical and economic constraints. Thus, monitoring of long-term trends through studies such as this can help identify ecosystems are returning to pre fire levels through natural recovery (e.g. species composition, spatial distribution of land cover) or if established rehabilitation programmes are meeting their desired targets. However it should be noted that remote sensing data should be assimilated with observations from field assignments to provide a comprehensive framework for post-fire rehabilitation planning.

#### Conclusions

This study was concerned with the quantification of the post-fire vegetation regeneration at the Okanagan Mountain Park, B.C., Canada, during an 8-years period, Canada following a fire event occurred in 2003 based on multi-temporal Landsat TM imagery analysis. In this framework, the spatio-temporal relationships between vegetation re-growth dynamics, topography and burn severity of the study area were also examined. Some key points from this study are the following:

- i) The use of NDVI to assess post-fire vegetation has been extensively examined, however far less research has concentrated on the use of RI as an alternative. Independent of possible radiometric calibration uncertainty, minor error in the atmospheric correction, topographic distortions, and phenological differences in vegetation, RI provides a more comprehensive index for quantifying the trends in post-fire

vegetation regeneration, and to some extent can provide validation for NDVI measurement in the absence of field data. Findings of the use of both indices showed a gradual to moderate recovery of vegetation in the studied region to the pre-fire conditions. Analysis of vegetation regeneration in the fire-affected area showed that fires have returned to around 60% of the pre-fire levels 8 years after fire suppression. Post-fire NDVI spatial patterns showed a relatively rapid regeneration in the initial year following the fire, with those becoming more gradual in subsequent years.

- ii) The spatial extent of the pre-fire vegetation was concentrated on the south eastern side of the burn scar. These areas were predominantly coniferous forests and grasslands on shallow south facing slopes. During analysis of regeneration in the subsequent image dates, initial (<4 years) regeneration was also more prominent in this area. Subsequent regeneration rates were highest on the low severity areas. These factors point to a spatial heterogeneity in vegetation and landscape response as a result of more localised factors. This more complex pattern of vegetation regeneration is also in good agreement with many studies (e.g. Inbar, Tamir, & Wittenberg, 1998; Turner et al. 1997).
- iii) Topography is a key control on burning severity and vegetation regeneration. Similar to other studies in the northern hemisphere, south facing exposures were most susceptible to burn and thus showed the highest burn severity (Karaman et al., 2011; Mouillot, Ratte, Joffre, Mouillot, & Rambal, 2005; Wimberly & Reilly, 2007). Aspect influences the fire proneness of an area due to the effect it has on insolation and evapotranspiration rates. Higher solar radiation values on south facing exposures increases the likelihood of ignition due to lower soil moisture content and drier environments and thus greater burn severity. Post-fire vegetation recovery also displays faster recovery rates on northern aspects due to more favourable moisture conditions (Karaman et al., 2011; Moreira et al., 2011; Mouillot et al., 2005).
- iv) To our knowledge, there are few studies to have examined the interrelationships of vegetation regeneration, topography and burn severity, especially in the case of a single large fire.

Although not comprehensive, results from this combination study show a promising avenue for a more extensive study of post-fire vegetation regrowth utilising remote sensing data in the possible absence of field data. Although an extensive initial recovery and rehabilitation programme was undertaken following the Okanagan Mountain Park Fire, results from this study suggest a potentially cost-effective method to evaluate post-fire damage, and monitor long-term vegetation recovery in the burned area. Information on the relationship between topography and burn severity could be utilised to analyse areas which are more susceptible to high severity burns, important information when considering areas for rehabilitation or the location of fire prevention measures. Results also corroborate the usefulness of EO as an optimum solution for an assessment of a restoration process following a fire event, at no cost and at regular time intervals. An understanding of the spatial and temporal patterns of vegetation re-growth dynamics from satellite imagery can assist to better appreciate post-fire landscape processes. It can also provide important support practically to the development of management systems to suppress and prevent fires; enable the definition of land use management rules and policies, or in the design and implementation of policies leading to specific landscape management goals. This is extremely important from a commercial perspective where prediction of variable postfire response across a disturbed landscape enables

managers to envision the rate of return of valuable goods and services. Furthermore, as was the case in our study, information on vegetation species composition and landscape patterns of recovery post-fire is vital for the preservation of local environments and habitats found in National Parks and protected ecosystems. Moreover, the long-term monitoring of such vegetation recovery dynamics can provide important information regarding recovery programmes and if they are indeed meeting their desired targets. Given the relatively straightforward integration of vegetation regrowth mapping methodologies with freely distributed continuous EO data, future efforts should be directed towards the operational development of products that can be used to support local studies of land cover restoration and burn severity mapping after wildfires.

## Acknowledgements

Authors are grateful to the United States Geological Survey (USGS), NASA and GeoBase for providing free access to the data used in the present study.

## References

- Agriculture and Agri-Food Canada. (2012). ISO 19131 land cover for agricultural regions of Canada, Circa 2000 – Data product specification [Online]. Available [http://www.agr.gc.ca/atlas/support/document\\_documentdesupport/circa2000Landcover/en/ISO\\_19131\\_Land\\_Cover\\_for\\_Agricultural\\_Regions\\_of\\_Canada\\_Circa\\_2000\\_Data\\_Product\\_Specification.pdf](http://www.agr.gc.ca/atlas/support/document_documentdesupport/circa2000Landcover/en/ISO_19131_Land_Cover_for_Agricultural_Regions_of_Canada_Circa_2000_Data_Product_Specification.pdf) Accessed 18.03.14.
- Arianoutsou, M., Christopoulou, A., Kazanis, D., Tountas, T., Ganou, E., Bazos, I., et al. (2010). Effects of fire on high altitude coniferous forests of Greece. In *6th international conference of wildland fire, Coimbra*.
- Arianoutsou, M., Gimeno, T., Kazanis, D., Pausas, J., & Vallejo, R. (2007). Characterization of fire vulnerable *Pinus halepensis* ecosystems in Spain and Greece'. In V. Leone, & R. Lovreglio (Eds.), *Proceedings of the International Workshop MED-PINE 3: Conservation, regeneration and restoration of mediterranean pines and their ecosystems* (pp. 131–142). Bari: CIHEAM (Options Méditerranéennes : Série A. Séminaires Méditerranéens; n. 75).
- Arno, S. F., Harrington, M. G., Fiedler, C. E., & Carlson, C. E. (1995). Restoring fire-dependent ponderosa pine forests in western Montana. *Ecological Restoration*, 13(1), 32–36.
- ASTER GDEM. (2009). ASTER GDEM version 1. Readme File <http://www.gdem.aster.ersdac.or.jp> Accessed 24.07.11.
- BC Ministry of Forest and Change. (2003). *Fire review summary for Okanagan Mountain Fire (K50628)* [pdf]. Available at [http://bcwildfire.ca/History/ReportsAndReviews/2003/Okanagan\\_Fire\\_Review\\_K50628.pdf](http://bcwildfire.ca/History/ReportsAndReviews/2003/Okanagan_Fire_Review_K50628.pdf) Accessed 11.07.13.
- Benson, R. E., & Green, A. W. (1987). *Colorado's timber resources. Resource Bulletin INT-48*. Ogden, UT: U.S. Department of Agriculture, Forest Service.
- Beschta, R. L., Rhodes, J. J., Kauffman, J. B., Gresswell, R. E., Minshall, G. W., Karr, J. R., et al. (2004). Postfire management on forested public lands of the western United States. *Conservation Biology*, 18(4), 957–967.
- Bowman, D. M., Balch, J. K., Artaxo, P., Bond, W. J., Carlson, J. M., Cochrane, M. A., et al. (2009). Fire in the earth system. *Science*, 324(5926), 481–484.
- Brewer, C. K., Winne, J. C., Redmond, R. L., Opitz, D. W., & Mangrich, M. V. (2005). Classifying and mapping wildfire severity. *Photogrammetric Engineering & Remote Sensing*, 71(11), 1311–1320.
- Burned Area Restoration. (2014). *National Parks services* [online]. Available at <http://www.nps.gov/fire/wildland-fire/resources/documents/burned-area-restoration.pdf> Accessed 05.11.14.
- Cannon, S. H., Gartner, J. E., Wilson, R. C., Bowers, J. C., & Laber, J. L. (2008). Storm rainfall conditions for floods and debris flows from recently burned areas in southwestern Colorado and Southern California. *Geomorphology*, 96(3), 250–269.
- Casady, G. M., Leeuwen, W. J. D., & Marsh, S. E. (2009). Evaluating post-wildfire vegetation regeneration as a response to multiple environmental determinants. *Environmental Model Assessment*, 15(5), 295–307.
- Cawson, J. G., Sheridan, G. J., Smith, H. G., & Lane, P. N. J. (2013). Effects of fire severity and burn patchiness on hillslope-scale surface runoff, erosion and hydrologic connectivity in a prescribed burn. *Forest Ecology and Management*, 310, 219–233.
- Cerdà, A., & Doerr, S. H. (2005). Influence of vegetation recovery on soil hydrology and erodibility following fire: an eleven year investigation. *International Journal of Wildfire*, 14(4), 423–437.
- Chen, S., Chen, L.-F., Liu, Q.-h., Li, X., & Tan, Q. (2005). Remote sensing and GIS-based integrated analysis of coastal changes and their impacts in Lingding Bay, Pearl River Estuary, South China. *Ocean & Coastal Management*, 48, 65–83.

- Cocke, A. E., Fulé, P. Z., & Crouse, J. E. (2005). Forest change on a steep mountain gradient after extended fire exclusion: San Francisco Peaks, Arizona, USA. *Journal of Applied Ecology*, 42, 814–823.
- Crutzen, P. J., & Andreae, M. O. (1990). Biomass burning in the tropics: impacts on atmospheric chemistry and bio-geochemical cycles. *Science*, 250, 1669–1678.
- D'Antonio, C. M., & Vitousek, P. M. (1992). Biological invasions by exotic grasses, the grass/fire cycle, and global change. *Annual Review of Ecology and Systematics*, 23(1), 63–87.
- De Santis, A., & Chuvieco, E. (2007). Burn severity estimation from remotely sensed data: performance of simulation versus empirical models. *Remote Sensing of Environment*, 108(4), 422–435.
- Díaz-Delgado, R., Lloret, F., Pons, X., & Terradas, J. (2002). Satellite evidence of decreasing resilience in Mediterranean plant communities after recurrent wildfires. *Ecology*, 83(8), 2293–2303.
- Díaz-Delgado, R., Salvador, R., & Pons, X. (1998). Monitoring of plant community regeneration after fire by remote sensing. In L. Traboud (Ed.), *Fire management and landscape ecology* (pp. 315–324). Fairfield, WA: International Association of Wildland Fire.
- Duffy, P. A., Epting, J., Graham, J. M., Rupp, T. S., & McGuire, A. D. (2007). Analysis of Alaskan burn severity patterns using remotely sensed data. *International Journal of Wildland Fire*, 16(3), 277–284.
- Epting, J., Verbly, D., & Sorbel, B. (2005). Evaluation of remotely sensed indices for assessing burn severity in interior Alaska using Landsat TM and ETM+. *Remote Sensing of Environment*, 96, 328–339.
- Exelis Visual Information Solutions. (2013). *FLAASH background* [online]. Available at <http://www.exelisvis.com/docs/BackgroundFLAASH.html> Accessed 21.07.13.
- Fox, D. M., Maselli, F., & Carrega, P. (2008). Using SPOT images and field sampling to map burn severity and vegetation factors affecting post forest fire erosion risk. *Catena*, 75(3), 326–335.
- Franks, S., Masek, J. G., & Turner, M. G. (2013). Monitoring forest regrowth following large scale fire using satellite data-A case study of Yellowstone National Park, USA. *European Journal of Remote Sensing*, 46, 551–569.
- Garcia, M. L., & Caselles, V. (1991). Mapping burns and natural reforestation using Thematic Mapper data. *Geocarto International*, 6(1), 31–37.
- Gouveia, C., DaCamara, C. C., & Trigo, R. M. (2010). Post-fire vegetation recovery in Portugal based on spot/vegetation data. *Natural Hazards and Earth System Science*, 544, 10(4), 673–684.
- Graham, R. T., McCaffrey, S., & Jain, T. B. (2004). *Science basis for changing forest structure to modify wildfire behavior and severity*. USDA Forest Service General Technical Report (p. 43). Ogden, Utah: RMRS-120, Rocky Mountain Research Station.
- Grissino-Mayer, H. D., & Swetnam, T. W. (2000). Century-scale climate forcing of fire regimes in the American Southwest. *The Holocene*, 10(2), 213–220.
- Hope, A., Albers, N., & Bart, R. (2012). Characterizing post-fire recovery of fynbos vegetation in the Western Cape Region of South Africa using MODIS data. *International Journal of Remote Sensing*, 33(4), 979–999.
- Hope, A., Tague, C., & Clark, R. (2007). Characterizing post-fire vegetation recovery of California chaparral using TM/ETM+ time-series data. *International Journal of Remote Sensing*, 28(6), 1339–1354.
- Huang, C., Song, K., Kim, S., Townshend, J. R. G., Davis, P., Masek, J. G., et al. (2008). Use of dark object concept and support vector machines to automate forest cover change analysis. *Remote Sensing of Environment*, 112, 970–985.
- Inbar, M., Tamir, M. I., & Wittenberg, L. (1998). Runoff and erosion processes after a forest fire in Mount Carmel, a Mediterranean area. *Geomorphology*, 24(1), 17–33.
- Intergovernmental Panel on Climate Change. (2007). Climate change 2007: Impacts, adaptation and vulnerability. In M. K. Parry, O. F. Canziani, J. P. Palutikof, P. J. van der Linden, & C. E. Hanson (Eds.), *Contribution of Working Group II to the fourth assessment report of the intergovernmental panel on climate change*. Cambridge, UK: Cambridge University Press.
- Intergovernmental Panel on Climate Change. (2011). Summary for policymakers. In C. B. Field, V. Barros, T. F. Stocker, D. Qin, D. Dokken, K. L. Ebi, et al. (Eds.), *Intergovernmental Panel on climate change special report on managing the risks of extreme events and disasters to advance climate change adaptation*. Cambridge, UK and New York, N.Y.: Cambridge University Press.
- Irons, J. (2011). *Landsat 7 science data user's handbook*. Report 430-15-01-003-0. National Aeronautics and Space Administration <http://landsathandbook.gsfc.nasa.gov/> Accessed 10.07.13.
- Jayen, K., Leduc, A., & Bergeron, Y. (2006). Effect of fire severity on regeneration success in the boreal forest of northwest Quebec, Canada. *Ecoscience*, 13(2), 143–151.
- Kalivas, D., Petropoulos, G. P., Athanasiou, I., & Kollias, V. (2013). An intercomparison of burnt area estimates derived from key operational products: analysis of Greek wildland fires 2005–2007. *Non-linear Processes in Geophysics*, 20, 1–13.
- Karaman, M., Özelen, E., & Ormeci, C. (2011). Determination of the forest fire potential by using remote sensing and geographical information system, case study-Bodrum/Turkey. In *Advances in Remote Sensing and GIS applications in Forest Fire Management from local to global assessments* (Vol. 51).
- Key, C. H., & Benson, N. C. (2005). Landscape assessment: ground measure of severity; the Composite Burn Index, and remote sensing of severity, the Normalized Burn Index. In D. Lutes, R. Keane, J. Caratti, C. Key, N. Benson, S. Sutherland, et al. (Eds.), *FIREMON: Fire effects monitoring and inventory system* (pp. 1–51). Forest Service, Rocky Mountains Research Station: USDA. General Technical Report RMRS-GTR-164-CD LA.
- Koutsias, N., Arianoutsou, M., Kallimanis, A. S., Mallinis, G., Halley, J. M., & Dimopoulos, P. (2012). Where did the fires burn in peloponnisos, greece the summer of 2007? Evidence for a synergy of fuel and weather. *Agricultural and Forest Meteorology*, 156(0), 41–53.
- Lentile, L. B., Morgan, P., Hudak, A. T., Bobbitt, M. J., Lewis, S. A., Smith, A. M. S., et al. (2007). Post-fire burn severity and vegetation response following eight large wildfires across the western United States. *Fire Ecology*, 3(1), 91–108.
- Lhermitte, S., Verbesselt, J., Verstraeten, W. W., & Coppin, P. (2007, July). Assessing vegetation regrowth after fire based on time series of SPOT-VEGETATION data. In *Analysis of multi-temporal remote sensing images, 2007* (pp. 1–7). IEEE. MultiTemp 2007. International Workshop on the.
- Lhermitte, S., Verbesselt, J., Verstraeten, W. W., & Coppin, P. (2010). A pixel based regeneration index using time series similarity and spatial context. *Photogrammetric Engineering & Remote Sensing*, 76(6), 673–682.
- Lhermitte, S., Verbesselt, J., Verstraeten, W. W., Veraverbeke, S., & Coppin, P. (2011). Assessing intra-annual vegetation regrowth after fire using the pixel based regeneration index. *ISPRS Journal of Photogrammetry and Remote Sensing*, 66(1), 17–27.
- Lunetta, R. S., Knight, J. F., Ediriwickrema, J., Lyon, J. G., & Worthy, L. D. (2006). Land-cover change detection using multi-temporal MODIS NDVI data. *Remote sensing of environment*, 105(2), 142–154.
- Malak, D. A., & Pausas, J. G. (2006). Fire regime and post-fire Normalised Difference Vegetation Index changes in the eastern Iberian peninsula (Mediterranean basin). *International Journal of Wildland Fire*, 15, 407–413.
- Marozas, V., Plausinyte, E., Augustaitis, A., & Kaciulyte, A. (2011). changes of ground vegetation and tree-ring growth after surface fires in scots pine forests. *Acta Biologica Universitatis Daugavpiliensis*, 11(2), 156–162.
- Marozas, V., Racinskas, J., & Bartkevicius, E. (2007). Dynamics of ground vegetation after surface fires in hemiboreal *Pinus sylvestris* forests. *Forest Ecology Management*, 250, 47–55.
- Maxwell, S. K., Airola, M., & Nuckles, J. R. (2010). Using Landsat satellite data to support pesticide exposure assessment in California. *International Journal of Health Geographics*, 9, 46.
- Miller, J. D., & Yool, S. R. (2002). Mapping forest post-fire canopy consumption in several overstory types using multi-temporal Landsat TM and ETM data. *Remote Sensing of Environment*, 82(2), 481–496.
- Minchella, A., Del Frate, F., Capogna, F., Anselmi, S., & Manes, F. (2009). Use of multitemporal SAR data for monitoring vegetation recovery of Mediterranean burned areas. *Remote Sensing Environment*, 113, 588–597.
- Moreira, F., Viedma, O., Arianoutsou, M., Curt, T., Koutsias, N., Rigolot, E., et al. (2011). Landscape–wildfire interactions in southern Europe: implications for landscape management. *Journal of Environmental Management*, 92(10), 2389–2402.
- Mouillot, F., Ratte, J. P., Joffre, R., Mouillot, D., & Rambal, S. (2005). Long-term forest dynamic after land abandonment in a fire prone Mediterranean landscape (central Corsica, France). *Landscape Ecology*, 20(1), 101–112.
- Mortsch, L. D. (2006). Impact of climate change on agriculture, forestry and wetlands. In J. Bhatty, R. Lal, M. Apps, & M. Price (Eds.), *Climate change and managed ecosystems* (pp. 45–67). Boca Raton, FL, USA: Taylor & Francis, CRC Press.
- Murphy, K. A., Reynolds, J. H., & Koltun, J. M. (2008). Evaluating the ability of the differenced Normalized Burn Ratio (dNBR) to predict ecologically significant burn severity in Alaskan boreal forests. *International Journal of Wildland Fire*, 17(4), 490–499.
- Naveh, Z. (1991). Mediterranean uplands as anthropogenic perturbation dependent systems and their dynamic conservation management. In O. Ravera (Ed.), *Terrrestrial and aquatic ecosystems: Perturbation and recovery* (pp. 545–557). New York: Ellis Horwood.
- Norton, J. (2006). *The use of remote sensing indices to determine wildland burn severity in Semiarid Sagebrush Steppe Rangelands using landsat ETM+ and SPOT 5*. Pocatello, ID: Idaho State University, 111 pp.
- Pausas, J. G., Llovet, J., Rodrigo, A., & Vallejo, R. (2008). Are wildfires a disaster in the Mediterranean Basin? – a review. *International Journal of Wildland Fire*, 17(6), 713–723.
- Pausas, J. G., Ribeiro, E., & Vallejo, R. (2004). Post-fire regeneration variability of *Pinus halepensis* in the eastern Iberian Peninsula. *Forest Ecology and Management*, 203(1), 251–259.
- Petropoulos, G. P., Griffiths, H. M., & Kalivas, D. P. (2014). Quantifying spatial and temporal vegetation recovery dynamics following a wildfire event in a Mediterranean landscape using EO data and GIS. *Applied Geography*, 50, 120–131.
- Petropoulos, G. P., & Kalaitzidis, C. (2011). Multispectral vegetation indices in remote sensing: an overview – book chapter (Chapter 2). In *Ecological modeling* (pp. 15–39). USA: Novapublishers, ISBN 978-1-61324-567-5.
- Petropoulos, G. P., Knorr, W., Scholze, M., Boschetto, L., & Karantounias, G. (2010). Combining ASTER multispectral imagery analysis and support vector machines for rapid and cost-effective post-fire assessment: a case study from the greek wildland fires of 2007. *Natural Hazards and Earth System Sciences*, 10, 305–317.
- Petropoulos, G. P., Kontoes, C., & Keramitsoglou, I. (2011). Burn area delineation from a uni-temporal perspective based on Landsat TM imagery classification using Support Vector Machines. *International Journal of Applied Earth Observation and Geoinformation*, 13(1), 70–80.
- Petropoulos, G. P., Kontoes, C. C., & Keramitsoglou, I. (2012). Land cover mapping with emphasis to burnt area delineation using co-orbital ALI and Landsat TM imagery. *International Journal of Applied Earth Observation and Geoinformation*, 18, 344–355. <http://dx.doi.org/10.1016/j.jag.2012.02.004>.
- Pettorelli, N., Vik, J. O., Mysterud, A., Gaillard, J.-M., Tucker, C. J., & Stenseth, N. C. (2005). Using the satellite-derived NDVI to assess ecological responses to environmental change. *Trends in Ecology and Evolution*, 20, 503–510.

- Pinno, B. D., Errington, R. C., & Thompson, D. K. (2013). Young jack pine and high severity fire combine to create potentially expansive areas of understocked forest. *Forest Ecology and Management*, 310, 517–522.
- Quayle, B., Brewer, K., & Williams, K. (2005). Monitoring post-fire vegetation recovery of wildland fire areas in the western United States using MODIS data. In *Proceedings of PECORA*.
- Rayne, S., Forest, K., & Friesen, K. J. (2009). *Projected climate change impacts on grape growing in the Okanagan Valley, British Columbia, Canada*. Nature Precedings. Rehabilitation and Recovery. (2014). National Parks services [online]. Available at <http://www.nps.gov/fire/wildland-fire/what-we-do/rehabilitation-and-recovery.cfm> Accessed 05.11.14.
- Riaño, D., Chuvieco, E., Salas, J., Palacios-Orueta, A., & Bastarrica, A. (2002). Generation of fuel type maps from Landsat TM images and ancillary data in Mediterranean ecosystems. *Canadian Journal of Forest Research*, 32(8), 1301–1315.
- Riaño, D., Chuvieco, E., Ustin, S., Zomer, R., Dennison, P., Roberts, D., et al. (2002). Assessment of vegetation regeneration after fire through multitemporal analysis of AVIRIS images in the Santa Monica Mountains. *Remote Sensing of Environment*, 79, 60–71.
- Robichaud, P. R., Lewis, S. A., Brown, R. E., & Ashmun, L. E. (2009). Emergency post-fire rehabilitation treatment effects on burned area ecology and long-term restoration. *Fire Ecology*, 5(1), 115–128. INTRODUCTION Wildland fires are natural earth system processes that have affected atmospheric composition, climate, and the evolution and spread of new plants and biomes for over, 350, 2.
- Roder, A., Hill, J., Duguy, B., Alloza, J. A., & Vallejo, R. (2008). Using long time series of Landsat data to monitor fire events and postfire dynamics and identify driving factors. A case study in the Ayora region (eastern Spain). *Remote Sensing Environment*, 112, 259–273.
- Rogers, B. M., Randerson, J. T., & Bonan, G. B. (2013). High-latitude cooling associated with landscape changes from North American boreal forest fires. *Biogeosciences*, 10(2), 699–718.
- Rouse, J. W., Haas, R. H., Schell, J. A., & Deering, D. W. (1973). *Monitoring vegetation systems in the great plains with ERTS Third ERTS Symposium*, NASA SP-351 (Vol. 1, pp. 309–317). Washington, DC: NASA.
- Schmidt, H., & Glasser, C. (1998). Multitemporal analysis of satellite data and their use in the monitoring of the environmental impacts of open cast lignite mining areas in eastern Germany. *International Journal of Remote Sensing*, 19, 2245–2260.
- Schroeder, W., Pereira, J. A. R., Morisette, J. T., Csizsar, I., Riggan, P., & Hoffman, J. W. (2002). A description of the “FireMapper™” airborne sensor validation campaigns in Brazil for quantifying the accuracy of MODIS fire products. *Earth Observer*, 14(6), 38–42.
- Shakesby, R. A., & Doerr, S. H. (2006). Wildfire as a hydrological and geomorphological agent. *Earth-Science Reviews*, 74(3), 269–307.
- Solans Vila, J. P., & Barbosa, P. (2010). Post-fire vegetation regrowth detection in the Deiva Marina region (Liguria-Italy) using Landsat TM and ETM+ data. *Ecological Modelling*, 221(1), 75–84.
- Soudani, K., Hmimina, G., Delpierre, N., Pontailler, J. Y., Aubinet, M., Bonal, D., et al. (2012). Ground-based Network of NDVI measurements for tracking temporal dynamics of canopy structure and vegetation phenology in different biomes. *Remote Sensing of Environment*, 123, 234–245.
- Song, C., Woodcock, C. E., & Li, X. (2002). The spectral/temporal manifestation of forest succession in optical imagery: The potential of multitemporal imagery. *Remote Sensing of Environment*, 82(2), 285–302.
- Song, C., & Woodcock, C. E. (2003). Monitoring forest succession with multitemporal Landsat images: factors of uncertainty. *Geoscience and Remote Sensing, IEEE Transactions on*, 41(11), 2557–2567.
- Stewart, S. I., Radeloff, V. C., & Hammer, R. B. (2003). Characteristics and location of the wildland–urban interface in the United States (CD-ROM) Track 4.A1. In *Proceedings of the second international wildland fire ecology and fire management workshop*. Boston: American Meteorological Society.
- Tachikawa, T., Hato, M., Kaku, M., & Iwasaki, A. (2011). *The characteristics of ASTER GDEM version 2, IGARSS*.
- The Atlas of Canada. (2009). *Productive Forest land use* [pdf]. Available at [http://atlas.nrcan.gc.ca/data/english/maps/forestry/productive\\_forest\\_land\\_use\\_map.pdf](http://atlas.nrcan.gc.ca/data/english/maps/forestry/productive_forest_land_use_map.pdf) Accessed 10.07.13.
- Turner, M. G., Dale, V. H., & Everham, E. H., III (1997). Fires, hurricanes, and volcanic canoes: comparing large disturbances. *BioScience*, 47(11), 758–768.
- USGS. (2004). FIREMON BR Cheat Sheet V4 [Online]. Available [http://burnseverity.cr.usgs.gov/pdfs/LAv4\\_BR\\_CheatSheet.pdf](http://burnseverity.cr.usgs.gov/pdfs/LAv4_BR_CheatSheet.pdf) Accessed 18.03.14.
- USGS. (2007). Burn severity overview – Applied remote sensing Principles [Online]. Available <http://burnseverity.cr.usgs.gov/overview/nbr/index.php> Accessed 18.03.14.
- Ustin, S. L., & Xiao, Q. F. (2001). Mapping successional boreal forests in interior central Alaska. *International Journal of Remote Sensing*, 22, 1779–1999.
- Van Wagendonk, J. W., Root, R. R., & Key, C. H. (2004). Comparison of AVIRIS and Landsat ETM+ detection capabilities for burn severity. *Remote Sensing of Environment*, 92(3), 397–408.
- Vapnik, V. (1995). *The nature of statistical learning theory*. New York, NY: Springer-Verlag.
- Veraverbeke, S., Somers, B., Gitas, I., Katagis, T., Polychronaki, A., & Goossens, R. (2012). Spectral mixture analysis to assess post-fire vegetation regeneration using landsat thematic mapper imagery: accounting for soil brightness variation. *International Journal of Applied Earth Observation and Geoinformation*, 14, 1–11.
- Viedma, O., Meliá, J., Segarra, D., & García-Haro, J. (1997). Modeling rates of ecosystem recovery after fires using Landsat TM data. *Remote Sensing of Environment*, 61, 383–398.
- Volpi, M., Petropoulos, G. P., & Kanevski, M. (2013). Flooding extent cartography with Landsat TM imagery and regularized kernel Fisher's discriminant analysis. *Computers and Geosciences*, 57, 24–31. <http://dx.doi.org/10.1016/j.cageo.2013.03.009>.
- Wallenius, T. H., Pitkänen, A., Kuuluvainen, T., Pennanen, J., & Karttunen, H. (2005). Fire history and forest age distribution of an unmanaged *Picea abies* dominated landscape. *Canadian Journal of Forest Research*, 35, 1540–1552.
- White, J. D., Ryan, K. C., Key, C. C., & Running, S. W. (1996). Remote sensing of forest fire severity and vegetation recovery. *International Journal of Wildland Fire*, 6(3), 125–136.
- Wimberly, M. C., & Reilly, M. J. (2007). Assessment of fire severity and species diversity in the southern Appalachians using Landsat TM and ETM+ imagery. *Remote Sensing of Environment*, 108(2), 189–197.
- Wittenberg, L., Malkinson, D., Beeri, O., Halutzy, A., & Tesler, N. (2007). Spatial and temporal patterns of vegetation recovery following sequences of forest fires in a Mediterranean landscape, Mt. Carmel Israel. *Catena*, 71(1), 76–83.
- Wulder, M. A., White, J. C., Cranny, M., Hall, R. J., Luther, J. E., Beaudoin, A., et al. (2008). Monitoring Canada's forests. Part 1: completion of the EOSD land cover project. *Canadian Journal of Remote Sensing*, 34(6), 549–562.

## Further reading

- Bisson, M., Fornaciai, A., Coli, A., Mazzarini, F., & Pareschi, M. T. (2008). The vegetation resilience after fire (VRAF) index: development, implementation and an illustration from central Italy. *International Journal of Applied Earth Observation and Geoinformation*, 10(3), 312–329.
- GeoBase. (2011). *Land cover, Circa 2000 – Vector* [online]. Available at <http://www.geobase.ca/geobase/en/data/landcover/index.html;jsessionid=310E4D3BCBA09BD5058C028ACF348E9Fgeobase1> Accessed 18.07.13.
- Justice, C. O., Malingreau, J. P., & Setzer, A. W. (1993). Satellite remote sensing of fire: potential and limitation. In P. Crutzen, & J. Goldammer (Eds.), *Fire in the environmental: The ecological, atmospheric, and climatic importance of vegetation fires* (pp. 77–88). New York: John Wiley and Sons.
- Koukoura, Z., Pappas, I. A., Kirkopoulos, C., & Karmiris, I. (2013). Effect of regional conditions on post-fire vegetation restoration rate in Mediterranean rangeland ecosystems. In *Dry grasslands of Europe: Grazing and ecosystem services* (Vol. 186).
- Pereira, J. M., Sá, A. C., Sousa, A. M., Silva, J. M., Santos, T. N., & Carreiras, J. M. (1999). Spectral characterization and discrimination of burnt areas. In Chuvieco (Ed.), *Remote sensing of large wildfires in the European mediterranean Basin* (pp. 122–138). Berlin/Heidelberg: Springer-Verlag.
- Sandink, D. (2008). *The resilience of the City of Kelowna: Exploring mitigation before, during and after the Okanagan Mountain Park Fire*. Institute for Catastrophic Loss Reduction.